and were then incubated in 40% sucrose: optimal cutting temperature (OCT) compound (1:1) overnight at 4°C. The testes were then embedded in OCT compound, frozen in liquid nitrogen, sectioned at 8-μm thickness on a cryostat (model 1720; Lietz, Wetzlar, Germany) and dried for 2 h. After wetting with PBS, the samples were treated with 0.1% Triton X-100 in PBS for 30 min and blocked with 5% normal goat serum and 3% BSA in PBS for 30 min. The samples were then incubated in rabbit polyclonal antibody, KP12 (4 μg/ml; Abcam, Cambridge, U.K.), in PBS at 4°C for 17 h. After washing with PBS, the testis sections were incubated with Alexa Fluor 546 goat anti-rabbit IgG (heavy-chain plus light-chain) (0.8 μg/ml; Molecular Probes, Eugene, OR) and Hoechst 33258 (10 μg/ml; Sigma–Aldrich, St. Louis, MO) for 30 min dissolved in PBS. After washing with PBS, the samples were analyzed with a BX50 microscope (Olympus, Tokyo, Japan) equipped with an imaging system composing of a CCD camera RETIGA Exi FAST 1394 and an imaging soft ware SlideBook 4 (Nippon Roper, Chiba, Japan).

Immunoblot Analysis. Tissue extracts were prepared and analyzed by immunoblotting with antibodies against Brek as described (3).

RT-PCR. Primers were checked by PCR to ensure that they generated single products of the predicted size. Primers for *Prm1*, *Prm2*, *TP1*, *TP2*, *CREM*, and *CaMK4* were kindly provided by A. Urano (University of Tokyo). PCR was performed at typical amplification parameters (95°C for 10 min, followed by 20–30 cycles of 95°C for 30 sec, 55°C for 30 sec, and 72°C for 1 min) by using Ex Taq (TaKaRa Biomedicals, Shiga, Japan) and ABI 9700 thermal cycler (Applied Biosystems, Foster City, CA).

Fractionation of the Normal Testicular Cells. Testes were collected from two male mice (8 weeks of age). The tunica albuginea was removed from each testis. The seminiferous tubules were placed in Eagle's Minimal Essential medium (GIBCO, Carlsbad, CA) containing 0.1% collagenase (Wako Pure Chemical Industries, Osaka, Japan), incubated at room temperature for 1 h with gentle swaying. The tubule suspension was transferred into a conical tube and kept standing for 5 min to precipitate tubule fragments. The supernatant containing separated cells was filtered through a nylon mesh and centrifuged at 600 × *g* for 10 min. The precipitant was used as a Leydig cell-rich fraction. The remaining tubules were dispersed by gentle pipetting a few times in PBS containing 1 mM EDTA to remove residual Leydig cells. Tubules were then treated with 0.25% Trypsin at 37°C for 10 min, and dispersed by vigorous pipetting. The suspension was filtrated through a nylon mesh and centrifuged at 600 × *g* for 10 min. The precipitant was dispersed in Eagle's Minimal Essential medium (pH 7.2) containing 10% FBS (GIBCO), transferred to gelatin-coated culture dishes, and incubated at 37°C for 2 h. The culture supernatant was filtered through a nylon mesh and centrifuged at 600 × *g* for 10 min. The precipitant was used as a germ cell-rich fraction. The cells attached to gelatin-coated culture dishes were washed with PBS a few times and then used as a Sertoli cell-rich fraction.

Assessment of Serum Hormone Levels. The bloods of 8-week-old male *Brek*$^{+/+}$ and *Brek*$^{-/-}$ mice were drawn by cardiocenthesis and incubated at 4°C overnight. After centrifugation at 800 × *g* for 10 min, the serum was collected and stored at −80°C until analysis. The levels of serum testosterone, luteinizing hormone, and follicle-stimulating hormone were measured by SRL, Tokyo, Japan.

Fertility Assessment. Eight-week-old *Brek*$^{+/-}$ and *Brek*$^{-/-}$ mice were intercrossed. One male was mated with two females for 2 weeks. Female mice were checked for vaginal plugs, and litter sizes were recorded.

Statistical Analysis. Student's *t* test for paired variables was used to examine differences, and data were considered significantly different at $P < 0.05$.

We thank Dr. A. Urano for primers for *Prm1*, *Prm2*, *TP1*, *TP2*, *CREM*, and *CaMK4* and Drs. S. Kina and T. Miyasaka for valuable discussion. This work was supported by grants-in-aid from the Ministry of Education, Culture, Sports, Science, and Technology of Japan.

1. Blume-Jensen P, Jiang G, Hyman R, Lee KF, O'Gorman S, Hunter T (2000) *Nat Genet* 24:157–162.
2. Robinson DR, Wu YM, Lin SF (2000) *Oncogene* 19:5548–5557.
3. Kawa S, Fujimoto J, Tezuka T, Nakazawa T, Yamamoto T (2004) *Genes Cells* 9:219–232.
4. Wang H, Brautigan DL (2002) *J Biol Chem* 277:49605–49612.
5. Kesavapany S, Lau KF, Ackerley S, Banner SJ, Shemilt SJ, Cooper JD, Leigh PN, Shaw CE, McLoughlin DM, Miller CC (2003) *J Neurosci* 23:4975–4983.
6. Reith AD, Rottapel R, Giddens E, Brady C, Forrester L, Bernstein A (1990) *Genes Dev* 4:390–400.
7. Meistrich ML (1977) *Methods Cell Biol* 15:15–54.
8. Gaozza E, Baker SJ, Vora RK, Reddy EP (1997) *Oncogene* 15:3127–3135.
9. Tomomura M, Hasegawa Y, Hashikawa T, Tomomura A, Yuzaki M, Furuichi T, Yano R (2003) *Brain Res Mol Brain Res* 112:103–112.
10. Raghunath M, Patti R, Bannerman P, Lee CM, Baker S, Sutton LN, Phillips PC, Damodar Reddy C (2000) *Brain Res Mol Brain Res* 77:151–162.
11. Tomomura M, Fernandez-Gonzales A, Yano R, Yuzaki M (2001) *Oncogene* 20:1022–1032.
12. Tomomura M, Furuichi T (2005) *J Biol Chem* 280:35157–35163.
13. Parvinen M, Pelto-Huikko M, Soder O, Schultz R, Kaipia A, Mali P, Toppari J, Hakovirta H, LonnerbSmeyne RJ, Klein R, *et al.* (1994) *Nature* 368:246–249.
14. Barbacid M (1994) *J Neurobiol* 25:1386–1403.
15. Nakamura T, Yao R, Ogawa T, Suzuki T, Ito C, Tsunekawa N, Inoue K, Ajima R, Miyasaka T, Yoshida Y, *et al.* (2004) *Nat Genet* 36:528–533.
16. Urano A, Endoh M, Wada T, Morikawa Y, Itoh M, Kataoka Y, Taki T, Akazawa H, Nakajima H, Komuro I, *et al.* (2005) *Mol Cell Biol* 25:6834–6845.
17. Weissenberg R, Eshkol A, Lunenfeld B (1982) *Arch Androl* 9:135–140.
18. Varmuza S, Jurisicova A, Okano K, Hudson J, Boekelheide K, Shipp EB (1999) *Dev Biol* 205:98–110.
19. Alessi D, MacDougall LK, Sola MM, Ikebe M, Cohen P (1992) *Eur J Biochem* 210:1023–1035.
20. Park C, Choi WS, Kwon H, Kwon YK (2001) *Mol Cells* 12:360–367.
21. Li C, Watanabe G, Weng Q, Jin W, Furuta C, Suzuki AK, Kawaguchi M, Taya K (2005) *Zoolog Sci* 22:933–937.
22. Feng C, Zhang J, Gasana V, Fu W, Liu Y, Zong Z, Yu B (2005) *Cell Biochem Funct* 23:415–420.
23. Huynh T, Mollard R, Trounson A (2002) *Hum Reprod Update* 8:183–198.
24. Fitch N, Richer CL, Pinsky L, Kahn A (1985) *Am J Med Genet* 20:31–42.

MOLECULAR AND CELLULAR BIOLOGY, Jan. 2006, p. 718–726 Vol. 26, No. 2
0270-7306/06/$08.00+0 doi:10.1128/MCB.26.2.718–726.2006

Oligo-Astheno-Teratozoospermia in Mice Lacking RA175/TSLC1/SynCAM/IGSF4A, a Cell Adhesion Molecule in the Immunoglobulin Superfamily

Eriko Fujita,[1] Yoriko Kouroku,[1] Satomi Ozeki,[1] Yuko Tanabe,[1] Yoshiro Toyama,[2] Mamiko Maekawa,[2] Naosuke Kojima,[3] Haruki Senoo,[3] Kiyotaka Toshimori,[2] and Takashi Momoi[1]*

Division of Differentiation and Development, Department of Inherited Metabolic Disorder, National Institute of Neuroscience, NCNP, Oawahigashi-machi 4-1-1, Kodaira, Tokyo 187-8502,[1] Department of Anatomy and Developmental Biology, Graduate School of Medicine, Chiba University, Inohana 1-8-1, Chiba, Chiba 260-8670,[2] and Department of Cell Biology and Histology, Akita University School of Medicine, 1-1-1, Hondo, Akita 010-8543,[3] Japan

Received 11 August 2005/Returned for modification 26 September 2005/Accepted 24 October 2005

RA175/TSLC1/SynCAM/IGSF4A (RA175), a member of the immunoglobulin superfamily with Ca^{2+}-independent homophilic *trans*-cell adhesion activity, participates in synaptic and epithelial cell junctions. To clarify the biological function of RA175, we disrupted the mouse *Igsf4a* (*Ra175/Tslc1/SynCam/Igsf4a Ra175*) gene. Male mice lacking both alleles of *Ra175* (*Ra175*$^{-/-}$) were infertile and showed oligo-astheno-teratozoospermia; almost no mature motile spermatozoa were found in the epididymis. Heterozygous males and females and homozygous null females were fertile and had no overt developmental defects. RA175 was mainly expressed on the cell junction of spermatocytes, elongating and elongated spermatids (steps 9 to 15) in wild-type testes; the RA175 expression was restricted to the distal site (tail side) but not to the proximal site (head side) in elongated spermatids. In *Ra175*$^{-/-}$ testes, elongated and mature spermatids (steps 13 to 16) were almost undetectable; round spermatids were morphologically normal, but elongating spermatids (steps 9 to 12) failed to mature further and to translocate to the adluminal surface. The remaining elongating spermatids at improper positions were finally phagocytosed by Sertoli cells. Furthermore, undifferentiated and abnormal spermatids exfoliated into the tubular lumen from adluminal surfaces. Thus, RA175-based cell junction is necessary for retaining elongating spermatids in the invagination of Sertoli cells for their maturation and translocation to the adluminal surface for timely release.

RA175/TSLC1/SynCAM/IGSF4A (RA175) is a new member of the immunoglobulin superfamily that has three immunoglobulin domains in its extracellular region and EYFI, a type II PDZ (postsynaptic density 95/disk large/zonula occluders-1)-binding domain, in its C-terminal intracellular region and has Ca^{2+}-independent homophilic *trans*-cell adhesion activity (10). RA175 was at first isolated as one of the genes preferentially expressed during the neuronal differentiation of P19 mouse embryonal carcinoma (P19 EC) cells induced by retinoic acid (9, 21) and is localized in the mouse developing nervous system and epithelium of various organs (2, 10, 11, 29). In the nervous system, RA175 is designated the synaptic cell adhesion molecule (SynCAM) and has been suggested to be involved in the formation of functional synapses (2). The localization of RA175 also suggests its biological role in the migration of neurons and the fasciculation of axons (11). In the developing lung epithelium, RA175 is localized in the cell-adherent region of the basolateral membrane in the polarized cells lining the lumen (10). Defects in *IGSF4A/tumor suppressor gene in lung cancer 1* (*TSLC1*), an orthologue of mouse *Igsf4a* (*Ra175*), promote the metastasis of lung carcinoma cells (18). However, little is known about its real biological function during organ development. To clarify the biological function of RA175, we disrupted the murine *Ra175* gene. Male mice lacking both alleles of *Ra175* (*Ra175*$^{-/-}$) were infertile, whereas heterozygous males and females and homozygous null females were fertile and had no overt developmental defects.

The junctional complex formed near the base of Sertoli cells is composed of ectoplasmic specialization and tight, gap, and desmosome-like junctions, and it divides the microenvironment into the basal and adluminal compartments (8). Spermatogonia and early spermatocytes, which are located in the basal compartment, are in contact with the basement membrane and Sertoli cells, whereas differentiating spermatocytes and spermatids, which are located in the adluminal compartment, are in contact with only Sertoli cells and therefore receive nutrition, hormones, and local factors exclusively from Sertoli cells.

Various cell adhesion molecules have been shown to be involved in the cell junction during spermatogenesis (3, 15, 16, 19, 22, 23). Among these, nectins and junctional adhesion molecule C (Jam-C)/Jam-3 (Jam-C), members of the immunoglobulin superfamily, have been shown to play essential roles in spermatogenesis (3, 15, 23). Poliovirus receptor-related 2 (pvrl2)/nectin-2 (nectin-2) and pvrl3/nectin-3 (nectin-3) are localized on the elongated spermatid (steps 9 to 16) and Sertoli cells, respectively, and form actin-based Sertoli-spermatid junctions that are involved in the assembly of actin filaments in the ectoplasmic specialization (26). Jam-C is localized on the round and elongated spermatids and mediates polarization of

* Corresponding author. Mailing address: Division of Differentiation and Development, Department of Inherited Metabolic Disorder, National Institute of Neuroscience, NCNP, Ogawahigashi-machi 4-1-1, Kodaira, Tokyo 187-8502, Japan. Phone: 81-42-341-2711. Fax: 81-42-346-1778. E-mail: momoi@ncnp.go.jp.

the adhesion junction with Sertoli cells by associating with partitioning-defective-3 (PAR-3) (15). Homozygous null males of *Nectin-2*$^{-/-}$ and *Jam-C*$^{-/-}$ are infertile (3, 15, 23). *Nectin-2*$^{-/-}$ male mice show a random disorganization of the spermatozoan head and midpiece due to overall disorganization of cytoskeletal structure, but they have motile spermatozoa (3, 23). *Jam-C*$^{-/-}$ male mice have an almost complete lack of elongated spermatids as a result of a defect in the polarization of adhesion junctions on the round spermatids, and they fail to produce mature sperm cells (15).

Here we show that *Ra175*$^{-/-}$ male mice are also infertile but have different phenotypes from *Nectin-2*$^{-/-}$ and *Jam-C*$^{-/-}$ male mice. They are defective in spermiogenesis, fail to produce mature sperm cells, and have severe oligo-astheno-teratozoospermia (low sperm number, low motility, and abnormal sperm morphology). In addition, we discuss the biological role of RA175 in spermiogenesis and the relationship between RA175 and other cell adhesion molecules.

MATERIALS AND METHODS

In situ hybridization. The EcoRI fragment of *RA175* in the pGEM-T easy vector was subcloned into pBluescript SK(+) vectors in both the sense and anti-sense orientations as previously described (29). Digoxigenin (DIG)-labeled *RA175* RNA probes were transcribed from XhoI-cut constructs using T3 RNA polymerase (DIG RNA Labeling kit T3; Boehringer Mannheim, Mannheim, Germany) in vitro according to the manufacturer's instructions. Frozen sections (10 μm thick) of mouse embryos at 13 embryonic days (E13.5) and testes of 4-week-old mice were treated with proteinase K (1 μg/ml) at 37°C for 10 min, refixed in 4% paraformaldehyde, and hybridized overnight with the DIG-labeled RNA probes. Hybridized RNA was detected using alkaline phosphatase-conjugated anti-DIG according to the procedure described by Wilkinson (31).

Generation of *Ra175*$^{-/-}$ mice. A 12-kb mouse *Igsf4a* (Mouse Genome Informatics accession no. 1889272, *Ra175*) genomic DNA fragment was cloned from the mouse 129Sv/Ev bacterial artificial chromosome genomic library. This genomic fragment contains exon 1 (13). The clone starts from 8.1 kb upstream of exon 1 and ends 3.8 kb downstream of exon 1, with a sequence of 5′-AATCTC TTATGTATAAAGCTGAAATGTACCAGG-3′. One side of the *lacZ-neo* gene cassette was inserted 5 bp upstream of the start ATG codon on exon 1. The sequence that was replaced starts with 5′-CCGACATGGCGAGTGCTGTGCT GCCGAGCGGATCCCAGTGTGCGGCGG-3′. The other side of the *lacZ-neo* gene cassette was inserted 2.4 kb downstream of exon 1 inside intron 1. The sequence that was replaced ends with 5′-TAGGGCTTGCTAAGACTCTCTCT CAAACTGTATAC-3′. In this strategy, the *lacZ-neo* cassette replaced the coding region of exon 1 and part of intron 1. As a result, the original *Ra175* promoter drives the LacZ expression. Ten micrograms of the targeting vector was linearized by NotI and then transfected by electroporation of 129 SvEv embryonic stem (ES) cells. After selection in G418 antibiotic, 300 surviving colonies were expanded for PCR analysis to identify recombinant clones.

To identify the wild-type and targeted alleles, primer pairs 5′-TGGCCCCTT CTAAGAAATACCCTC-3′ and 5′-GATTTGTAGCGAGGGAATGAGATGA C-3′ at 2.3 kb downstream of exon 1 and 5′-CCCAATAAGTCTCATAGAAC TGATTGTC-3′ and 5′-TGCGAGGCCAGAGGCCACTTGTGTAGC-3′ primers at the 5′ end of the Neo cassette were used for PCR analysis, respectively. The PCR amplified the 1.8-kb fragment for wild-type allele and 1.6-kb fragments for targeted allele at 94°C for 20 s, 62°C for 60 s, and 72°C for 120 s for 35 cycles, and then 72°C for 10 min. The correctly targeted ES cell lines were microinjected into the C57BL/6J blastocysts, and the chimeras were then set up for mating with the C57BL/6J mice, and they gave germ line transmission of the mouse *Ra175lacZ* knock-in gene. We intercrossed heterozygous *Ra175* mice to produce homozygous *Ra175*$^{-/-}$ mice.

X-Gal staining of mouse testis. LacZ activity in *Ra175*$^{-/-}$ testes was detected by 5-bromo-4-chloro-3-indolyl-β-D-galactopyranoside (X-Gal) staining as previously described (25). Mouse testes 10 to 12 weeks after birth were embedded in freezing medium and frozen on dry ice. The embedded testes were sectioned at a 15 μm thickness at −15°C. Each section was transferred onto a silanized slide and allowed to dry and fixed in a fixing solution (0.2% glutaraldehyde, 2 mM $MgCl_2$, and 5 mM EGTA in phosphate-buffered saline [PBS]). After being washed three times in a washing solution (2 mM $MgCl_2$, 0.01% sodium deoxycholate, and 0.02% Nonidet P-40 in PBS), each section was stained in the X-Gal staining solution [1 mg/ml X-Gal, 5 mM $K_3Fe(CN)_6$, 5 mM $K_4Fe(CN)_6$, and 2 mM $MgCl_2$ in PBS] at 30°C overnight. After being stained, testes were washed and stored in PBS.

Sperm count and motility analysis. We placed cauda epididymides in 0.1 ml of motile buffer (120 mM NaCl, 5 mM KCl, 25 mM $NaHCO_3$, 1.2 mM KH_2PO_4, 1.2 mM $MgSO_4$, and 1.3 mM $CaCl_2$). We minced the tissue with scissors and incubated it at 37°C for 5 min to allow sperm dispersal. The supernatant was obtained as a sperm suspension, and the motility of sperm in the suspension was visually monitored under phase-contrast images (IM type; Olympus, Tokyo, Japan). After 25-fold and/or 50-fold dilution, the number of sperm in the 0.1-μl suspension was counted by using cell counter plates under the microscope.

Immunohistochemical staining. Antibodies against a peptide corresponding to the C-terminal region of RA175 were prepared as previously described (10) and were used for the immunostaining. Testes of 10- to 12-week-old *Ra175*$^{+/+}$ and *Ra175*$^{-/-}$ male mice were fixed in 4% paraformaldehyde in phosphate-buffered saline (PBS) at 4°C overnight and then soaked in 30% sucrose-PBS at 4°C overnight and embedded in optimal cutting temperature compound (Sakura Finetec. Co., Ltd., Tokyo, Japan) and frozen. Frozen sections (10 μm thick) were cut on a cryostat and attached to Matsunami adhesive silane-coated slides (Matsunami Glass Co., Osaka, Japan) and incubated with rabbit anti-RA175 in PBS containing 0.1% skim milk and 0.1% Triton X-100 at 4°C for 2 days as described previously (10). Anti-RA175 immunoreactivity was detected using anti-rabbit immunoglobulin G-Alexa Fluor 568 (Molecular Probes, Eugene, OR). Acrosome structure was detected using fluorescein isothiocyanate-conjugated peanut agglutinin (PNA) (J-Oilmills, Tokyo, Japan) staining in place of *p*-aminosalicylic acid staining. F-actin was detected using Alexa Flour 568-phalloidin (Molecular Probes). Nuclei were detected by Hoechst 33342 dye at 37°C for 15 min. The sperm tail was detected by Alexa Fluor 568 Mitotracker (Molecular Probes). Immunoreactivity was viewed using a confocal laser-scanning microscope (CSU-10; Yokogawa, Tokyo, Japan).

Conventional light microscopy. We fixed testes of male mice (10 to 12 weeks of age) in Bouin or 4% paraformaldehyde neutral buffer solution, embedded them in paraffin, and cut 8-μm sections on a microtome. We stained sections with hematoxylin and eosin by standard procedures.

Conventional transmission electron microscopy. Adult mice (12 to 16 weeks of age) were perfusion fixed through the left ventricle with 3% glutaraldehyde in HEPES buffer (10 mM HEPES ethansulfanic acid [Nacalai Tesque, Kyoto, Japan] containing 145 mM NaCl). Testes cut into small pieces were immersed in the same fixative for an additional 2 h. The samples were then postfixed in 1% OsO_4 for 1 h. After routinely dehydrated with graded ethanol series, the samples were embedded in Epon812 and the ultrathin sections were made on an ultramicrotome (Ulreacut E; Reihert-jung, Vienna, Austria). The thin sections were stained with uranyl acetate and lead citrate and observed with a JEM 1200 EX (JEOL, Tokyo, Japan) transmission electron microscope. One-micrometer semithin sections were stained with toluidine blue for light microscopy.

RESULTS

To make clear the relationship between the biological function of RA175 and organ development, we examined the expression of *Ra175* mRNA in mouse embryos. In situ hybridization showed that *Ra175* mRNA was expressed in the nervous tissues including brain, spinal cord, and dorsal root ganglia (Fig. 1A and B) as well as in various epithelia, including hair follicles (Fig. 1B and C), lung epithelium (Fig. 1D), esophagus epithelium (Fig. 1E), olfactory epithelium (Fig. 1F), and tongue epithelium (Fig. 1G) in mouse embryos at embryonic day 13.5 (E13.5). It was also expressed in testes 4 weeks after birth (Fig. 1H) in spermatocytes and spermatids.

To determine the biological function of RA175, we inactivated *Ra175* in mouse ES cells by replacing exon 1 of the *Ra175* gene with the *lacZ* reporter gene cassette (Fig. 2A). Cell lines that had undergone a targeting event were used to generate mice that transmitted the disrupted gene. These mice were mated to produce *Ra175*$^{+/-}$ mice. Intercrosses yielded offspring (~20 litters) that segregated with the expected Mendelian frequency: 41 wild type, 101 heterozygotes (*Ra175*$^{+/-}$), and 42 homozygotes (*Ra175*$^{-/-}$) by PCR analysis (Fig. 2B).

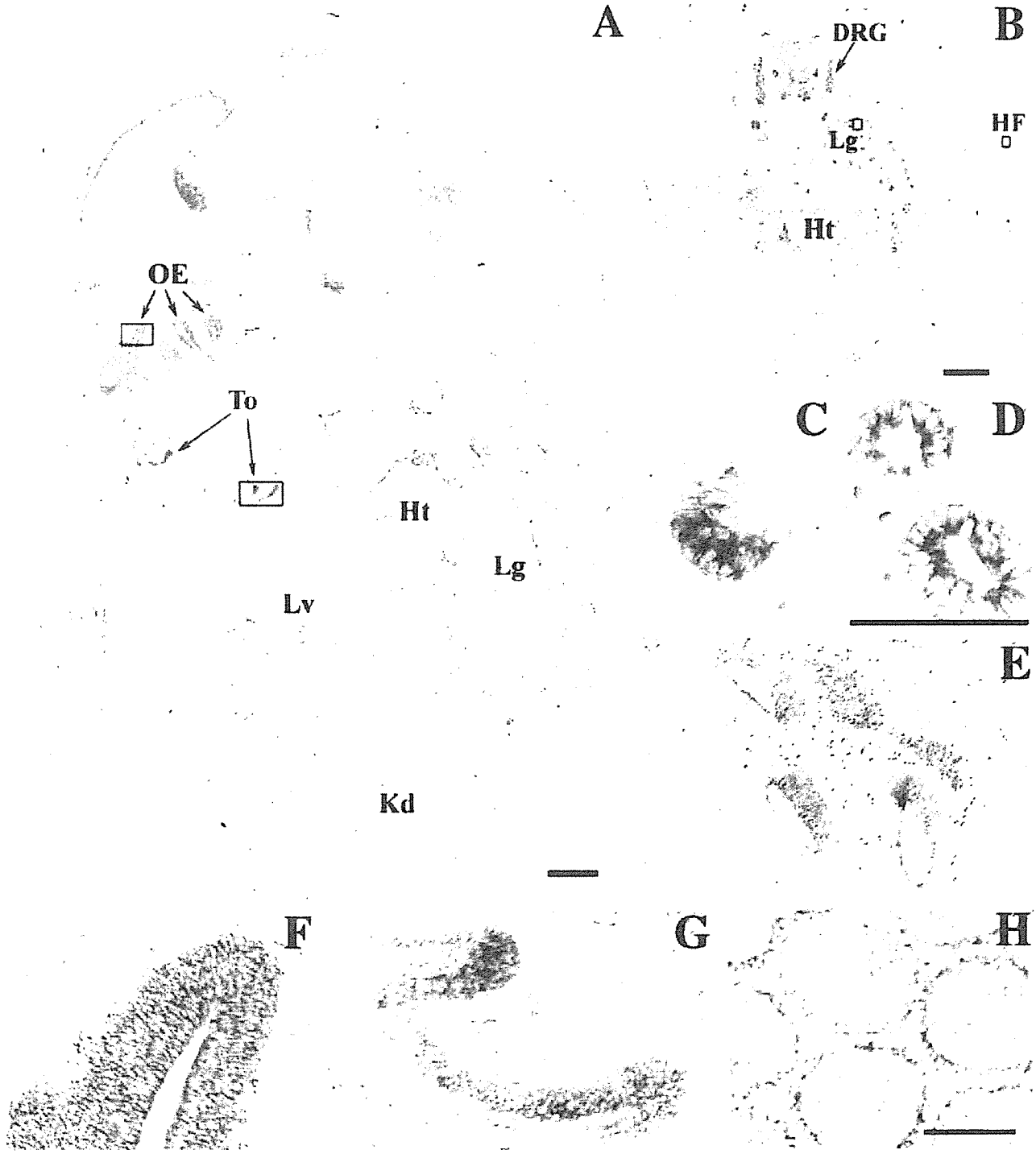

FIG. 1. In situ hybridization analysis of the expression of *Ra175* mRNA in mouse embryos and testes. Expression of the *Ra175* mRNA on the sagittal section (A) and transverse section of trunks (B) of mouse embryo at E13.5. (C to G) Magnification of the epithelium of each organ in the rectangular region in panels A and B. (C) Hair follicle; (D) lung; (E) esophagus; (F) olfactory epithelium; (G) tongues epithelium; (H) testis of the 4-week-old mouse. OE, olfactory epithelium; To, tongue; Lg, lung; Lv, liver; Kd, kidney; Ht, heart; DRG, dorsal root ganglia; HF, hair follicle. In addition to the nervous system including brain, spinal cord, and dorsal root ganglia, *Ra175* mRNA was detected in the various epithelium of the developing organs. Bars in panels A and B, 500 μm. Bars in panels C to H, 200 μm.

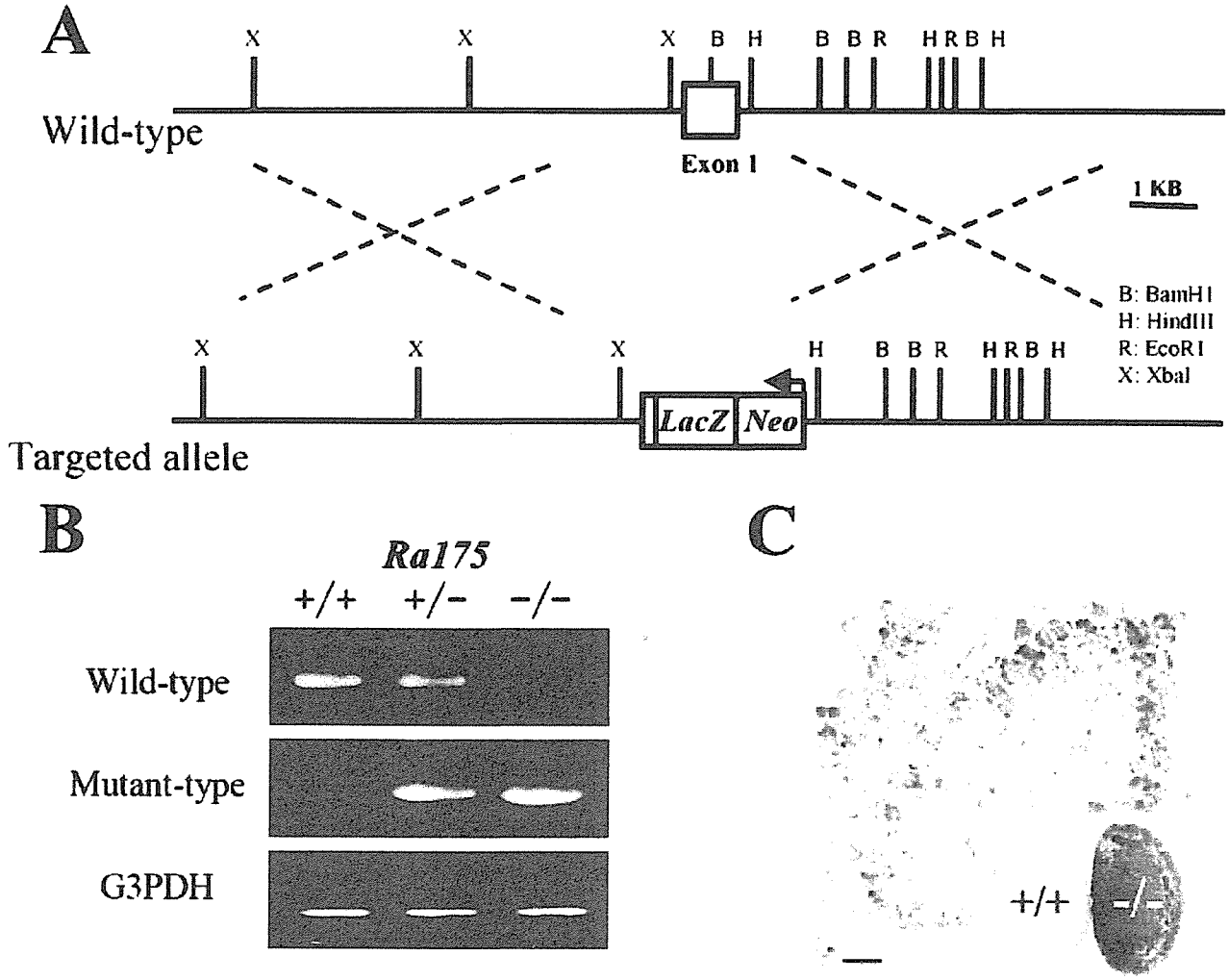

FIG. 2. Targeted disruption of the mouse *Ra175* gene. (A) Structure of the wild-type allele and the targeted allele. Exon 1 of the *Ra175* gene was replaced by *lacZ* and *neo* genes as described in Materials and Methods. (B) Genotype analysis of wild-type, heterozygote, and homozygote mice by PCR. (C) X-Gal staining of $Ra175^{+/+}$ and $Ra175^{-/-}$ testes. LacZ activity was detected in the germ cells including spermatocytes. Bar, 10 μm.

Male mice lacking both alleles of *Ra175* ($Ra175^{-/-}$) were infertile, while $Ra175^{+/-}$ males and females and $Ra175^{-/-}$ females were fertile. $Ra175^{-/-}$ mice had no overt developmental defects in the nervous tissues or other tissues except for in testes. Consistent with the finding of *Ra175* mRNA expression in the wild-type testes (Fig. 1H), LacZ activity was detected in the germ cells including spermatocytes in $Ra175^{-/-}$ testes but not in $Ra175^{+/+}$ testes (Fig. 2C).

The weight of $Ra175^{-/-}$ testes was about 15% lower than that in the wild-type ($Ra175^{+/+}$) animals. In severe cases, most spermatozoa were lost in the seminiferous tubules of the $Ra175^{-/-}$ mice, and only a small number remained (Fig. 3A). These remaining spermatozoa did not have motility (Fig. 3B). Thus, $Ra175^{-/-}$ males show oligo-asthenozoospermia (low sperm number and low motility).

A detailed histological analysis of seminiferous tubules from $Ra175^{-/-}$ mice clearly showed that in contrast with $Ra175^{+/+}$ (Fig. 4A and C), residual bodies and the midpieces of sperm

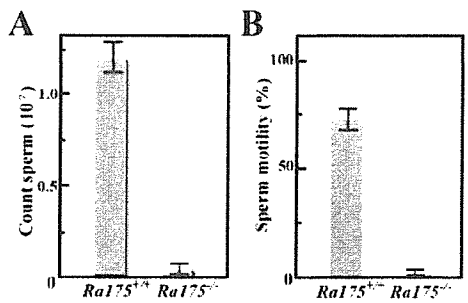

FIG. 3. Number of spermatozoa and the motility of $Ra175^{+/+}$ and $Ra175^{-/-}$ mice. The number of spermatozoa (A) from $Ra175^{+/+}$ and $Ra175^{-/-}$ mice and their motility (B). Normal and abnormal cells with nuclei were counted as spermatozoa. The value is the average of three experiments. $Ra175^{-/-}$ males show low sperm number and motility. Error bars indicate standard deviation. Statistical significance ($P < 0.05$) in each assay was assessed by Student's *t* test.

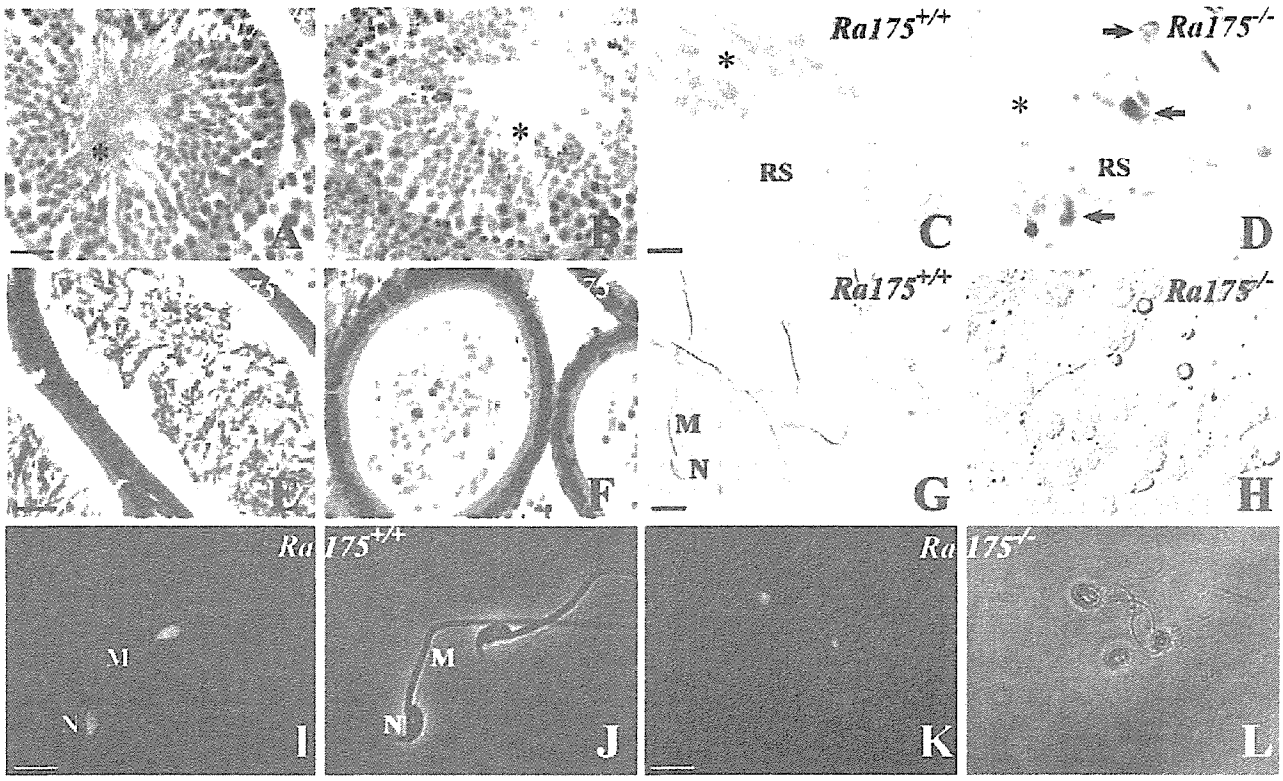

FIG. 4. Spermatogenesis at stage VIII and germ cells in the cauda epididymidis of *Ra175*$^{+/+}$ and *Ra175*$^{-/-}$. (A, C, E, G, I, and J) *Ra175*$^{+/+}$; (B, D, F, H, K, and L) *Ra175*$^{-/-}$; (A, B, E, and F) hematoxylin and eosin (HE) staining; (C and D) toluidine blue staining; (G and H) Nomarski images; (I and K) fluorescence images with Mitotracker staining for mitochondria (red) and Hoechst staining for the nucleus (blue); (J and L) bright-field images. Compared to normal spermatogenesis in *Ra175*$^{+/+}$ testes (A and C), spermatogenesis normally proceeds until the round spermatid stage (B and D), but abnormally shaped germ cells appear in elongating stages (B) in *Ra175*$^{-/-}$ testes. In contrast with *Ra175*$^{+/+}$ testes (A and C), the areas for the residual bodies and the thick portions of spermatid tails (mitochondrial regions indicated by asterisks) are almost absent in *Ra175*$^{-/-}$ testes (B and D). In contrast with *Ra175*$^{+/+}$ (E, G, I, and J), mature spermatozoa are not detected, but many exfoliated germ cells are detected in the cauda epididymal lumen of *Ra175*$^{-/-}$ (F, H, K, and L). Note that thick portions (mitochondrial regions) are absent in the exfoliated elongated spermatid tails in the *Ra175*$^{-/-}$ (H, K, and L). Thus, immature elongated spermatids in the *Ra175*$^{-/-}$ cauda epididymidis lacked mitochondrial region, which eventually leads to sterility. RS, round spermatids; M, middle piece; N, nucleus. Arrows indicate irregular nuclei. Bars in panels A, B, E, and F, 20 μm. Bars in panels C and D, 5 μm. Bars in panels G to L, 10 μm.

tails (asterisk) were almost not present in *Ra175*$^{-/-}$ testes (Fig. 4B and D). Round spermatids were morphologically normal, but elongated spermatids showed abnormally shaped heads in *Ra175*$^{-/-}$ testes, and they were not localized at the adluminal surface. Furthermore, very few morphologically mature elongated spermatids were detected in *Ra175*$^{-/-}$ testes (Fig. 4B and D). Thus, germ cells differentiated normally into the round spermatid stage but abnormally into the elongated spermatid stage.

Germ cells including round spermatids exfoliated at various stages of differentiation in *Ra175*$^{-/-}$ testes and were found in the lumen of the cauda epididymides (Fig. 4E to L). The remaining spermatozoa had irregularly shaped heads, abnormally arranged mitochondria (Fig. 4K and L), and erroneously attached flagella (unpublished observation) as well as round heads, probably due to the abnormal differentiation from round spermatids (Fig. 4H). Thus, *Ra175*$^{-/-}$ males showed oligo-astheno-teratozoospermia (low sperm number, low motility, and abnormal sperm morphology) leading to sterility.

We examined the localization of RA175 during spermiogenesis. The stage of spermatid differentiation is closely associated with changes in the acrosomal system. Localization of RA175

TABLE 1. Localization of RA175 during spermiogenesis classified by PNA and acrosomal structure[a]

Spermiogenesis stage (step)	PNA	RA175
Round spermatids (1 to 5)	+ (acrosomal granules)	±
Round spermatids (6 to 8)	+ (cap acrosome)	±
Elongating spermatid (9 to 12)	+ (flattened cap acrosomis)	+ (mostly distal site)
Elongated spermatid (13 to 15)	−	+ (only distal site)
Mature spermatid (16)	−	−

[a] The normal spermatid differentiation of the wild type are mainly classified into five groups by PNA staining and acrosomal structures as follows: (i) Round spermatids (steps 1 to 5); PNA-positive acrosomal granules and RA175-weakly positive. (ii) Round spermatid (steps 6 to 8); PNA-positive cap formation of acrosome and RA175-weakly positive. (iii) Elongating spermatid (steps 9 to 12); PNA-positive flattened cap formation of acrosome and RA175 is positive on the cell junction of the distal site and a few proximal head portion. (iv) Elongated spermatid (steps 13 to 15); PNA-negative and RA175 is positive on the cell junction of the distal site (tail side) but negative on the proximal site (head site). (v) Mature spermatid (step 16); RA175-negative, no residual bodies.

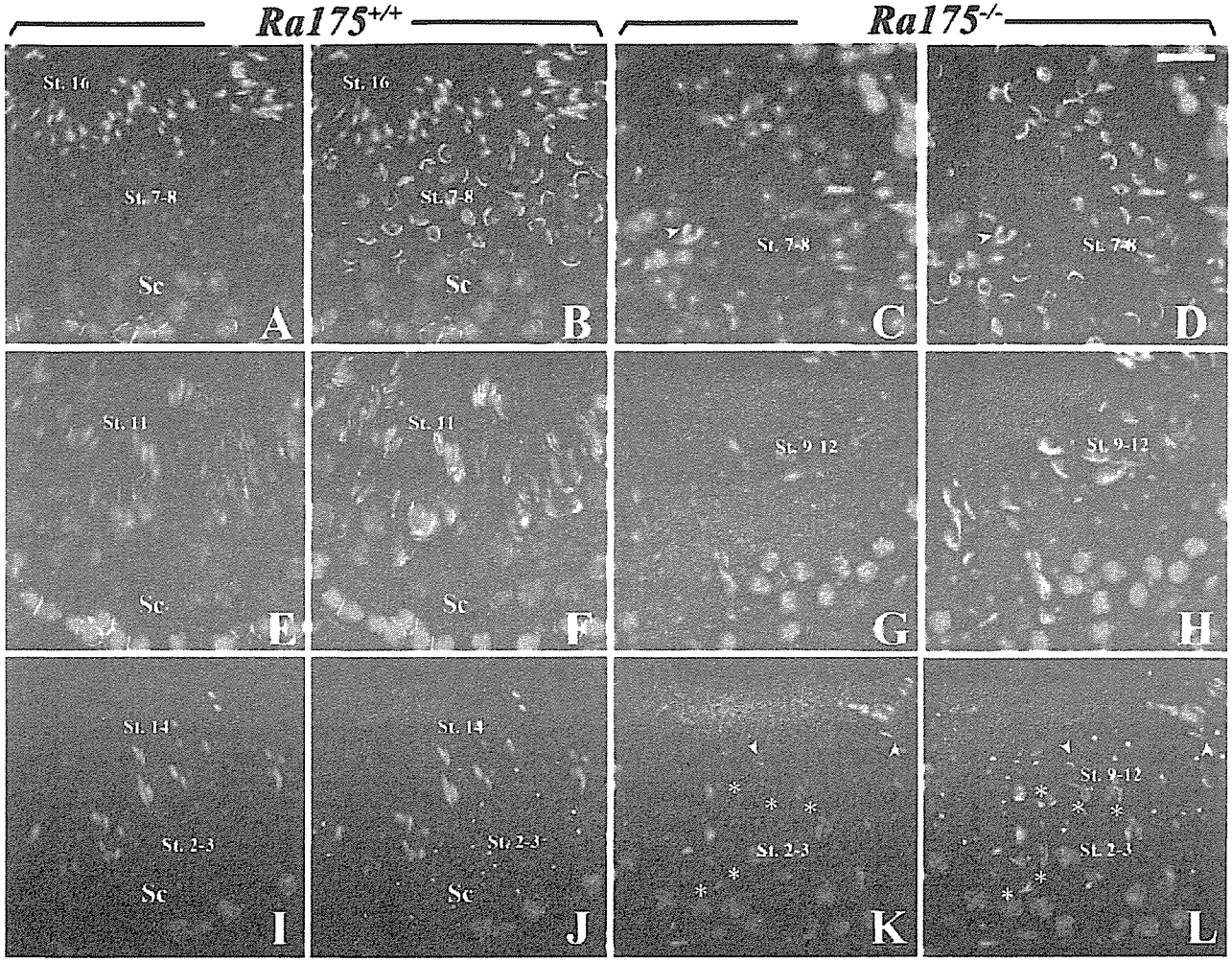

FIG. 5. Localization of RA175 during the differentiation from round to elongated spermatids in *Ra175*$^{+/+}$ and *Ra175*$^{-/-}$ testes. (A, B, E, F, I, and J) *Ra175*$^{+/+}$; (C, D, G, H, K, and L) *Ra175* $^{-/-}$. (A, C, E, G, I, and K) Merged images of spermatids stained with anti-RA175 (red) and Hoechst staining (blue). (B, D, F, H, J, and L) Merged images of spermatids stained with anti-RA175 (red), fluorescein isothiocyanate-conjugated PNA (green), and Hoechst staining (blue). (A to D) Stage VII; (E to H) stage XI; (I and J) stages II and III; (K and L) stages XII to II/III. Steps of the spermiogenesis of *Ra175*$^{-/-}$ testes were not exactly determined due to abnormal differentiation and lack of elongated spermatids. The differentiation of round to elongated spermatids was assessed by PNA staining (Table 1), which recognizes the acrosomal structure. Spermiogenesis normally occurs in *Ra175*$^{+/+}$ testes, whereas in *Ra175*$^{-/-}$ testes, PNA-positive elongating spermatids (steps 9 to 12; asterisks in K and L) appear but stay together with the PNA-positive round spermatid (steps 2 and 3; K and L), probably due to the translocation failure. Elongated spermatids (steps 13 to 15) were almost not detected in *Ra175*$^{-/-}$ testes (arrowheads in panels C, D, K, and L). St., step; Sc, spermatocytes. Bar, 20 μm.

during spermiogenesis (steps 1 to 16) could be mainly classified into five groups by peanut agglutinin (PNA) staining (Table 1), which recognizes the Golgi and acrosomal structures (15). In addition to the cell junctions between Sertoli cells and spermatocytes (Fig. 5A, B, E, F, I, and J), RA175 was strongly expressed in the cell junction of the elongating (step 11 in Fig. 5E and F) and elongated spermatids (step 14 in Fig. 5I and J) but weakly expressed on the round spermatids (steps 7 and 8 in Fig. 5A and B and steps 2 and 3 in Fig. 5I and J). In the elongating (steps 9 to 12) and elongated spermatid (steps 13 and 14), RA175 was mainly localized on the cell junctions of the distal site (Fig. 5E, F, I, and J) and tail side of elongated spermatids that faced to the lumen of tubules at stages XI to VI. After displacement of residual bodies, RA175 reactivity was remarkably reduced in the mature spermatids (step 16 in Fig. 5A and B).

PNA staining confirmed that acrosome formation of the round spermatid (steps 6 to 8) was not compromised in *Ra175*$^{-/-}$ testes (Fig. 5C and D). The elongating spermatids (steps 9 to 12) also appeared (Fig. 5G and H), but the elongated spermatids (PNA negative; steps 13 to 16) were hardly detected at the adluminal surface or other sites (arrowheads in Fig. 5C, D, K, and L). The elongating spermatids failed to proceed into further maturation steps and were not translocated to the adluminal surface. The remaining elongating spermatids (asterisks in Fig. 5K and L) decreased in their cell number but stayed together with the round spermatids (steps 1 to 5), which appeared in the same region (Fig. 5L).

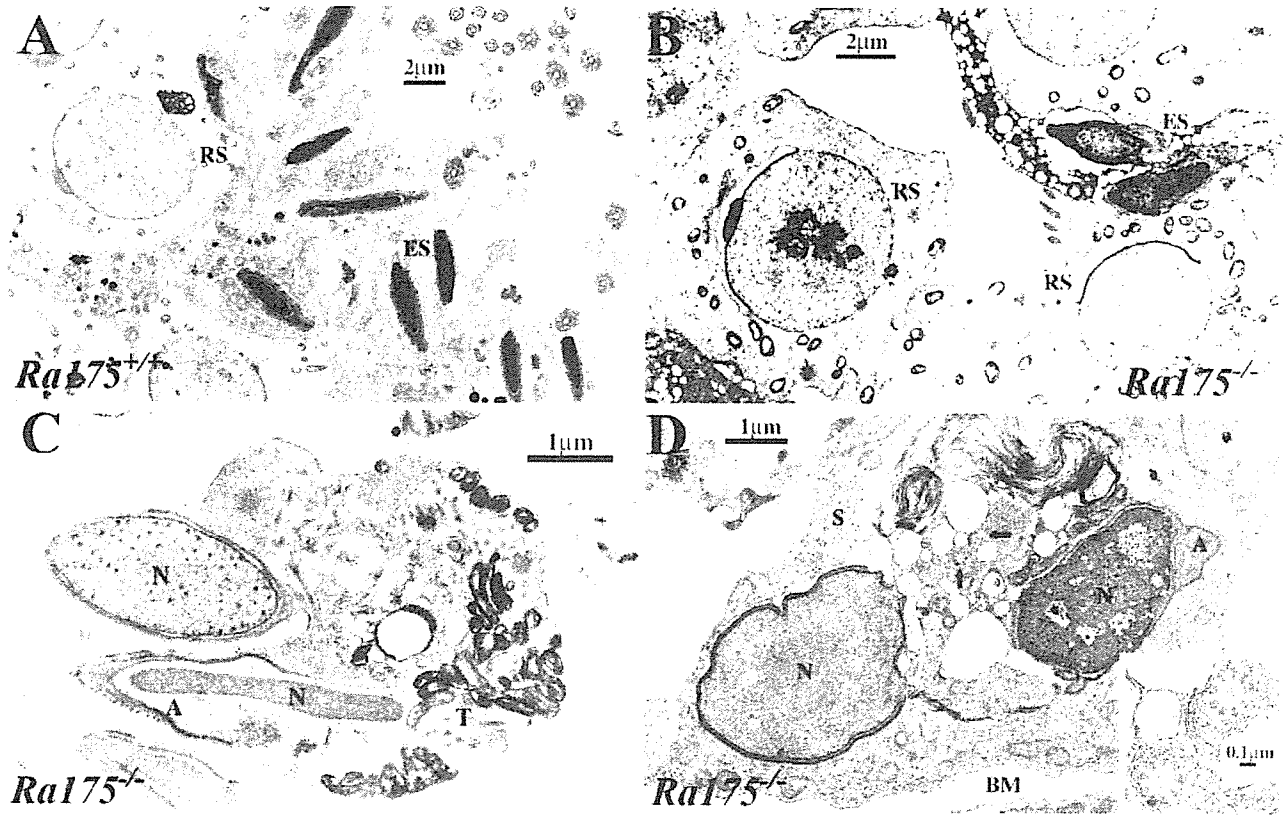

FIG. 6. Electron micrographs showing normal spermatogenesis in *Ra175*$^{+/+}$ testes and abnormal spermatogenesis in *Ra175*$^{-/-}$ testes. All germ cell images are taken from seminiferous tubules at around stage VIII. Compared to *Ra175*$^{+/+}$ (A), *Ra175*$^{-/-}$ germ cells (B) are capable of developing normally to round spermatid (RS) stage, whereas elongating spermatids start to degenerate and form irregular nuclei with incomplete condensation (ES in panel B). (C) Elongating spermatids are frequently formed as a symplast in which malformed sperm components are found; e.g., incompletely condensed nuclei (N), incompletely developed acrosome (A), and disorganized tail components (T). (D) Degenerated germ cells, which have ill-formed nuclei (N), acrosome (A), and axoneme (arrows), are readily phagocytosed by Sertoli cells. Inset, higher magnification of axoneme (arrowed area). BM, basement membrane.

Thus, the steps of the spermiogenesis were disturbed in *Ra175*$^{-/-}$ testes.

Electron microscopy analyses clarified that compared to the normal spermatogenesis in *Ra175*$^{+/+}$ testes (Fig. 6A), round spermatids developed normally and formed acrosomes, but the condensation of elongated spermatids was incomplete in *Ra175*$^{-/-}$ testes (Fig. 6B). Symplasts, which are formed by undivided elongating spermatids, were frequently formed, and they contained ill-formed sperm components such as incompletely condensed nuclei, abnormally formed acrosomes, and disorganized tail components (Fig. 6C). Interestingly, degenerated spermatids, which had ill-condensed nuclei, unusually shaped acrosomes, and disarranged tail components, were readily phagocytosed by Sertoli cells (Fig. 6D). Owing to this, the number of elongating spermatids was reduced, eventually leading to oligozoospermia. Thus, *Ra175*$^{-/-}$ spermatocytes could normally differentiate into the round spermatids but failed to differentiate into the elongated spermatids.

DISCUSSION

The phenotypic difference between *Ra175*$^{-/-}$ and *Rxrb*$^{-/-}$ or *Cnot7*$^{-/-}$ mice showing oligo-astheno-teratozoospermia. The *Ra175*$^{-/-}$ male mice were infertile due to the oligo-astheno-teratozoospermia. Some gene-targeted mice have been shown to be positive for oligo-astheno-teratozoospermia. Retinoic acid receptor-α (RARα) and retinoid X receptor-β (RXRβ) signals are essential for spermatogenesis. Male mice lacking RXRβ (*Rxrb*$^{-/-}$) and Cnot (*Cnot7*$^{-/-}$), a regulator of transcriptional function of RXRβ, are sterile due to an abnormal process of germ cell maturation that leads to oligo-astheno-teratozoospermia (17, 24). RA175 is at first isolated as the gene highly expressed during the differentiation of P19 EC cells induced by retinoic acid (9, 21, 29), making it possible to speculate that the deficiency of the RAR/RXR receptor signal leads to a lack of *Ra175* expression, resulting in a defect of spermatid-Sertoli cell junctions, which leads to abnormal spermiogenesis.

However, there is a remarkable morphological difference between *Ra175*$^{-/-}$ and *Rxrb*$^{-/-}$ or *Cnot7*$^{-/-}$ testes. In the *Rxrb*$^{-/-}$ and *Cnot7*$^{-/-}$ mutants, there is a progressive accumulation of lipids within the Sertoli cells and many terminal deoxynucleotidyltransferase-mediated dUTP-biotin nick end labeling-positive (apoptotic) cells in testes, and their seminiferous tubules contain degraded mature spermatids at

stages IX to XI as well as residual nuclear fragments at all the other stages (14, 20, 24). In contrast, a progressive accumulation of lipids and terminal deoxynucleotidyltransferase-mediated dUTP-biotin nick end labeling-positive cells was not detected (unpublished data), and elongated spermatids were almost not present in *Ra175*$^{-/-}$ testes. These phenotypic differences between *Ra175*$^{-/-}$ and *Rxrb*$^{-/-}$ or *Cnot7*$^{-/-}$ testes suggest that genes other than *Ra175* are also involved in the defect of spermiogenesis in *Rxrb*$^{-/-}$ or *Cnot7*$^{-/-}$ testes.

Oligo-astheno-teratozoospermia and defects in the elongating spermatid in the *Ra175*$^{-/-}$ mice. Light and electron microscopic analyses clearly showed that in *Ra175*$^{-/-}$ testes, germ cells normally differentiated into round spermatids but did not differentiate into mature elongated spermatids (Fig. 4 to 6); elongating spermatids (steps 9 to 12) were observed, but they failed to mature further. Thus, lack of mature elongated spermatid in *Ra175*$^{-/-}$ testes is one of the major causes for the oligo-astheno-teratozoospermia. In addition, the undifferentiated germ cells, including round spermatids and abnormally differentiated spermatids located at the adluminal surface, seem to exfoliate into the seminiferous tubular lumen, probably due to a weak association between the spermatids and Sertoli cells or denaturation of the abnormal and undifferentiated spermatids. Furthermore, Sertoli cells, similar to the residual bodies, may phagocytose the abnormally differentiated spermatids, which were not translocated to the adluminal surface. This possibility is supported by facts that the cell number of the remaining elongating spermatids decreased (asterisks in Fig. 5K and L) and that the phagocytosis of the abnormal elongated spermatids by Sertoli cells was frequently observed (Fig. 6D). Thus, deficiency of RA175 causes loss of the elongated and mature spermatids (steps 13 to 16) and the exfoliation and phagocytosis of the abnormal or undifferentiated elongated spermatids, leading to oligo-teratozoospermia. In addition, only a few spermatozoa found in the epididymis were immotile (Fig. 3). Owing to this, *Ra175*$^{-/-}$ male mice display oligo-atsheno-teratozoospermia and become sterile.

The phenotypic difference between *Ra175*$^{-/-}$ and *Nectin-2*$^{-/-}$ or *Jam-C*$^{-/-}$ mice. Until now, many genes of cell adhesion molecules in the immunoglobulin superfamily including nectin-2 and JAM-C have been disrupted (3, 4, 5, 12, 15, 23). Among them, *Jam-C*$^{-/-}$ and *Nectin-2*$^{-/-}$ male mice are infertile.

In *Jam-C*$^{-/-}$ testes, the differentiation of elongated spermatid is inhibited. Jam-C proteins, which have important functions in the assembly of tight junctions in endothelial and epithelial cells (1), are localized in most generations of spermatogenic cells, including round and elongated spermatids (15). Jam-C is confined to the junctional plaques in the heads of elongated spermatids and alters the adhesion structures, polarizing the localization of PAR-3 and anchoring spermatids to the Sertoli cell epithelium. Round spermatids in *Jam-C*$^{-/-}$ testes lack acrosomal structures and are defective in the polarization of the adhesion structures. This inhibits the differentiation of round spermatids into elongated spermatids (15).

In contrast with *Jam-C*$^{-/-}$ testes, the acrosomal structures of the round spermatids were uncompromised in *Ra175*$^{-/-}$ testes (Fig. 5 and 6). *Ra175*$^{-/-}$ germ cells can apparently and normally differentiate into the round spermatids with acrosomal structure. Furthermore, the level of the Jam-C was almost equal in *Ra175*$^{+/+}$ and *Ra175*$^{-/-}$ testes (unpublished data). Thus, lack of RA175 does not seem to affect the level of Jam-C, which provides the polarization of junctional plaque on the elongated spermatids.

However, Jam-C has a type II PDZ binding domain, which binds to polarizing proteins such as PAR-3 via PDZ domains (6, 7, 28). Since RA175 also has type II PDZ binding motifs at C terminals (2, 10), it may be possible that the lack of interaction between RA175 and proteins containing PDZ domains causes the change of the Jam-C distribution or localization on the elongated spermatid, providing the abnormal polarization or absence of junctional plaque, which induces the abnormal interaction between spermatid and Sertoli cells and results in the defect of the differentiation into the elongated spermatid. This possibility remains to be studied.

Nectin-2$^{-/-}$ male mice show a random disorganization of the spermatozoan head and midpiece due to overall disorganization of cytoskeletal structure, but they still possess motile spermatozoa (3, 23). The spermatid (steps 9 to 15) forms a Sertoli-spermatid junction via heterophilic interaction between nectin-2 and nectin-3 (23, 26). The association of the C termini of nectins and afadin, an actin-binding protein, is thought to participate in the assembly of actin filaments at the apical ectoplasmic specialization.

The following results suggest the distinct roles of the RA175 and nectins in the elongating spermatids. (i) Localization of RA175 on the elongated spermatid (steps 13 to 15) was restricted more distal to the head, near the tail (Fig. 5 and Table 1), whereas nectin-3 and nectin-2 are still restricted to around the head region of the elongated spermatid (26). (ii) There is the phenotypical difference between *Nectin-2*$^{-/-}$ and *Ra175*$^{-/-}$ mice. A deficiency in nectin-2 causes cytoskeletal disruption, resulting in the malformation of spermatids, but it does not induce the loss of the elongated spermatids or oligo-astheno-teratozoospermia (3, 23), while nectin-mediated spermatid-Sertoli cell junction and the cytoskeletal organization structure were normal; however, there was no maturation and no translocation of the elongated spermatid in *Ra175*$^{-/-}$ testes (unpublished data). Thus, RA175- and nectin-mediated cell junctions seem to have distinct roles in the distal portion and proximal portion in the spermatid-Sertoli cell junctions, respectively.

Possible roles of RA175-mediated cell junction in the distal portion of the elongated spermatids. Light and electron microscopical analyses (Fig. 5 and 6) clearly showed that in *Ra175*$^{-/-}$ testes, the elongating spermatids (steps 9 to 12) are defective and fail to proceed into the further maturation step, while *Ra175*$^{-/-}$ Sertoli cells seem to be normal; the lack of cell contact of the elongating spermatid with Sertoli cells in their invagination results in the incomplete differentiation, no maturation, and no translocation of the elongating spermatids.

Recently, in addition to TSLC1 and SynCAM, RA175 has been designated IGSF4A, SgIGSF, and Necl-2 (27, 30), which have been isolated from various tissues and cells, suggesting that RA175 has diverse biological functions in various tissues. However, both male and female *Ra175*$^{-/-}$ mice have not shown any altered behavior, including reproductive behavior and any incidence of tumor for almost 1 year. Furthermore, *Ra175*$^{-/-}$ mice had no overt developmental defects in tissues other than testes, suggesting that RA175-mediated cell junc-

tion is very essential for spermatogenesis in testes. Normally, the elongated spermatid is captured in the invagination of the Sertoli cells during displacement of the spermatid cytoplasm from the condensing nuclei during steps 13 to 15 (8). During these processes, the elongated spermatid receives the nutrition, hormones, and local factors required for maturation exclusively from the surrounding Sertoli cells. After this, it is translocated and released to the tubular lumen from the adluminal surface.

Defect of *IGSF4* (*TSLC1*), human orthologue of *Igsf4a* (*Ra175*), promotes the metastasis of lung carcinoma cells (18), suggesting that loss of RA175 makes the cells easily release from cell-to-cell interaction in some of the organs. It is likely that lack of RA175-mediated cell interaction makes the elongated spermatid and Sertoli cell adhesion unstable. Thus, RA175-mediated cell junction in the distal site retains the elongated spermatids in the invaginations of Sertoli cells until release as spermatozoa.

In conclusion, our results indicate that the RA175-based cell junction is necessary for anchoring the elongating spermatids to Sertoli cells. This specialization retains the elongated spermatid in the invagination of Sertoli cells during their complete differentiation and mediates the translocation of the elongated spermatids to the adluminal surface.

ACKNOWLEDGMENTS

We thank Shigeki Yuasa for valuable scientific discussion and Hisae Kikuchi for technical advice.

This work was supported in part by Grants-in-Aid from the Ministry of Education, Science and Culture of Japan and by Research Grant 14A-1 for Nervous and Mental Disorders and Research on Brain Science from the Ministry of Health and Welfare of Japan, the Human Science Foundation. E.F. and Y.K. are Research Fellows of the Japan Society for the Promotion of Science.

REFERENCES

1. **Aurrand-Lions, M., L. Duncan, C. Ballestrem, and B. A. Imhof.** 2001. JAM-2, a novel immunoglobulin superfamily molecule, expressed by endothelial and lymphatic cells. J. Biol. Chem. **276:**2733–2741.
2. **Biederer, T., Y. Sara, M. Mozhayeva, D. Atasoy, X. Liu, E. T. Kavalali, and T. C. Sudhof.** 2002. SynCAM, a synaptic adhesion molecule that drives synapse assembly. Science **297:**1525–1531.
3. **Bouchard, M. J., Y. Dong, B. M. McDermott, Jr., D. H. Lam, K. R. Brown, M. Shelanski, A. R. Bellve, and V. R. Racaniello.** 2000. Defects in nuclear and cytoskeletal morphology and mitochondrial localization in spermatozoa of mice lacking nectin-2, a component of cell-cell adherence junctions. Mol. Cell. Biol. **20:**2865–2873.
4. **Cremer, H., R. Lange, A. Christoph, M. Plomann, G. Vopper, J. Roes, R. Brown, S. Baldwin, P. Kraemer, S. Scheff, D. Barthels, K. Rajewsky, and W. Wille.** 1994. Inactivation of the N-CAM gene in mice results in size reduction of the olfactory bulb and deficits in spatial learning. Nature **367:**455–459.
5. **Dahme, M., U. Bartsch, R. Martini, B. Anliker, M. Schachner, and N. Mantei.** 1997. Disruption of the mouse L1 gene leads to malformations of the nervous system. Nat. Genet. **17:**346–349.
6. **Ebnet, K., A. Suzuki, S. Ohno, and D. Vestweber.** 2004. Junctional adhesion molecules (JAMs): more molecules with dual functions? J. Cell Sci. **117:**19–29.
7. **Ebnet, K., M. Aurrand-Lions, A. Kuhn, F. Kiefer, S. Butz, K. Zander, M. K. Meyer zu Brickwedde, A. Suzuki, B. A. Imhof, and D. Vestweber.** 2003. The junctional adhesion molecule (JAM) family members JAM-2 and JAM-3 associate with the cell polarity protein PAR-3: a possible role for JAMs in endothelial cell polarity. J. Cell Sci. **116:**3879–3891.
8. **Fawcett, D. W.** 1986. A textbook of histology, p. 796–850. *In* W. Bloom and D. W. Fawcett (ed.), Male reproductive system, Saunders Company, Philadelphia, Pa.
9. **Fujita, E., A. Soyama, K. Urase, T. Mukasa, and T. Momoi.** 1998. RA175, which is expressed during the neuronal differentiation of P19 EC cells, temporally expressed during neurogenesis of mouse embryos. Neurosci. Res. **22:**283.
10. **Fujita, E., A. Soyama, and T. Momoi.** 2003. RA175, which is the mouse orthologue of TSLC1, a tumor suppressor gene in human cancer, is a cell adhesion molecule. Exp. Cell. Res. **287:**57–66.
11. **Fujita, E., K. Urase, A. Soyama, Y. Kouroku, and T. Momoi.** 2005. Distribution of RA175/TSLC1/SynCAM, a member of the immunoglobulin superfamily, in the developing nervous system. Dev. Brain Res. **154:**199–209.
12. **Fukamauchi, F., O. Aihara, Y. J. Wang, K. Akasaka, Y. Takeda, M. Horie, H. Kawano, K. Sudo, M. Asano, K. Watanabe, and Y. Iwakura.** 2001. TAG-1-deficient mice have marked elevation of adenosine A1 receptors in the hippocampus. Biochem. Biophys. Res. Commun. **281:**220–226.
13. **Fukami, T., H. Satoh, E. Fujita, T. Maruyama, H. Fukuhara, M. Kuramochi, S. Takamoto, T. Momoi, and Y. Murakami.** 2002. Identification of the Tslc1 gene, a mouse orthologue of the human tumor suppressor TSLC1 gene. Gene **295:**7–12.
14. **Gehin, M., M. Mark, C. Dennefeld, A. Dierich, H. Gronemeyer, and P. Chambon.** 2002. The function of TIF2/GRIP1 in mouse reproduction is distinct from those of SRC-1 and p/CIP. Mol. Cell. Biol. **22:**5923–5937.
15. **Gliki, G., K. Ebnet, M. Aurrand-Lions, B. A. Imhof, and R. H. Adams.** 2004. Spermatid differentiation requires the assembly of a cell polarity complex downstream of junctional adhesion molecule-C. Nature **431:**320–324.
16. **Goossens, S., and F. van Roy.** 2005. Cadherin-mediated cell-cell adhesion in the testis. Front. Biosci. **10:**398–419.
17. **Kastner, P., M. Mark, M. Leid, A. Gansmuller, W. Chin, J. M. Grondona, D. Decimo, W. Krezel, A. Dierich, and P. Chambon.** 1996. Abnormal spermatogenesis in RXR beta mutant mice. Genes Dev. **10:**80–92.
18. **Kuramochi, M., H. Fukuhara, T. Nobukuni, T. Kanbe, T. Maruyama, H. P. Ghosh, M. Pletcher, M. Isomura, M. Onizuka, T. Kitamura, T. Sekiya, R. H. Reeves, and Y. Murakami.** 2001. TSLC1 is a tumor-suppressor gene in human non-small-cell lung cancer. Nat. Genet. **27:**427–430.
19. **Lui, W. Y., D. Mruk, W. M. Lee, and C. Y. Cheng.** 2002. Sertoli cell tight junction dynamics: their regulation during spermatogenesis. Biol. Reprod. **68:**1087–1097.
20. **Mascrez, B., N. B. Ghyselinck, M. Watanabe, J. S. Annicotte, P. Chambon, J. Auwerx, and M. Mark.** 2004. Ligand-dependent contribution of RXR beta to cholesterol homeostasis in Sertoli cells. EMBO Rep. **5:**285–290.
21. **McBurney, M. W., E. M. Jones-Villeneuve, M. K. Edwards, and P. J. Anderson.** 1982. Control of muscle and neuronal differentiation in a cultured embryonal carcinoma cell line. Nature **299:**165–167.
22. **Mruk, D. D., and C. Y. Cheng.** 2004. Cell-cell interactions at the ectoplasmic specialization in the testis. Trends Endocrinol. Metab. **15:**439–447.
23. **Mueller, S., T. A. Rosenquist, Y. Takai, R. A. Bronson, and E. Wimmer.** 2003. Loss of nectin-2 at Sertoli-spermatid junctions leads to male infertility and correlates with severe spermatozoan head and midpiece malformation, impaired binding to the zona pellucida, and oocyte penetration. Biol. Reprod. **69:**1330–1340.
24. **Nakamura, T., R. Yao, T. Ogawa, T. Suzuki, C. Ito, N. Tsunekawa, K. Inoue, R. Ajima, T. Miyasaka, Y. Yoshida, A. Ogura, K. Toshimori, T. Noce, T. Yamamoto, and T. Noda.** 2004. Oligo-astheno-teratozoospermia in mice lacking Cnot7, a regulator of retinoid X receptor beta. Nat. Genet. **36:**528–533.
25. **Ozaki, H., Y. Watanabe, K. Takahashi, K. Kitamura, A. Tanaka, K. Urase, T. Momoi, K. Sudo, J. Sakagami, M. Asano, Y. Iwakura, and K. Kawakami.** 2001. Six 4, a putative myogenin gene regulator, is not essential for mouse embryonal development. Mol. Cell. Biol. **21:**3343–3350.
26. **Ozaki-Kuroda, K., H. Nakanishi, H. Ohta, H. Tanaka, H. Kurihara, S. Mueller, K. Irie, W. Ikeda, T. Sakai, E. Wimmer, Y. Nishimune, and Y. Takai.** 2002. Nectin couples cell-cell adhesion and the actin scaffold at heterotypic testicular junctions. Curr. Biol. **12:**1145–1150.
27. **Shingai, T., W. Ikeda, S. Kakunaga, K. Morimoto, K. Takekuni, S. Itoh, K. Satoh, M. Takeuchi, T. Imai, M. Monden, and Y. Takai.** 2003. Implications of nectin-like molecule-2/IGSF4/RA175/SgIGSF/TSLC1/SynCAM1 in cell-cell adhesion and transmembrane protein localization in epithelial cells. J. Biol. Chem. **278:**35421–35427.
28. **Suzuki, A., C. Ishiyama, K. Hashiba, M. Shimizu, K. Ebnet, and S. Ohno.** 2002. aPKC kinase activity is required for the asymmetric differentiation of the premature junctional complex during epithelial cell polarization. J. Cell Sci. **115:**3565–3573.
29. **Urase, K., A. Soyama, E. Fujita, and T. Momoi.** 2001. Expression of RA175 mRNA, a new member of immunoglobulin super family, in developing mouse brain. NeuroReport **12:**3217–3221.
30. **Watabe, K., A. Ito, Y. I. Koma, and Y. Kitamura.** 2003. IGSF4: a new intercellular adhesion molecule that is called by three names, TSLC1, SgIGSF and SynCAM, by virtue of its diverse function. Histol. Histopathol. **18:**1321–1329.
31. **Wilkinson, D. G.** 1992. Whole mount in situ hybridization of vertebrate embryos, p. 75–83. *In* D. G. Wilkinson (ed.), In situ hybridization: a practical approach, Oxford IRL Press, New York, N.Y.

ELSEVIER

Journal of Reproductive Immunology xxx (2007) xxx–xxx

JOURNAL OF REPRODUCTIVE IMMUNOLOGY

www.elsevier.com/locate/jreprimm

Expression of toll-like receptors 2, 3, 4, and 9 genes in the human endometrium during the menstrual cycle

Tetsuya Hirata, Yutaka Osuga*, Kahori Hamasaki, Yasushi Hirota, Emi Nose, Chieko Morimoto, Miyuki Harada, Yuri Takemura, Kaori Koga, Osamu Yoshino, Toshiki Tajima, Akiko Hasegawa, Tetsu Yano, Yuji Taketani

Department of Obstetrics and Gynecology, Faculty of Medicine, University of Tokyo, 7-3-1 Hongo, Bunkyo-ku, Tokyo 113-8655, Japan

Received 31 May 2006; received in revised form 10 November 2006; accepted 15 November 2006

Abstract

Innate immunity in the endometrium has fundamental significance for reproduction. Although toll-like receptors (TLRs) play central roles in innate immune responses, their expression in the human endometrium remains to be fully elucidated. We have examined the gene expression of TLR2, TLR3, TLR4, and TLR9 in endometrial tissues by real-time quantitative PCR and *in situ* hybridization. The expression levels of the four genes in endometrial tissues varied in a similar pattern during the menstrual cycle: the levels were high in the perimenstrual period and low in the periovulatory period. Expression of the four genes was detected in both epithelial cells and stromal cells throughout the menstrual cycle. Expression levels were higher in epithelial cells for TLR3 and in stromal cells for TLR4, while they were comparable in epithelial cells and stromal cells for TLR2 and TLR9. These findings imply that differential spatio-temporal expression patterns of TLRs subserve proper innate immunity of the endometrium.

Keywords: Toll-like receptor; Endometrium; Expression; *In situ* hybridization

1. Introduction

The endometrium is a pivotal component of the reproductive organs, which nourishes implanting embryos. However, it is vulnerable to the spread of microorganisms from the vagina and cervix, resulting in endometrial infection that may impair normal fecundity. Thus, protective mechanisms against unwanted infection should be inherent in the endometrium to achieve successful reproduction.

Toll-like receptors (TLRs) are central regulators of innate immune responses (Takeda et al., 2003). Currently, 10 different human TLRs have been described, and each TLR recognizes distinct pathogen-associated molecular patterns. TLRs are thought to be important for host defense against external pathogens in mucosal systems, such as the intestinal and respiratory tracts. We have previously demonstrated the presence and possible implication of TLR4, a receptor for LPS, in the human endometrium (Hirata et al., 2005).

Other TLRs have also been shown to be present in the human endometrium. Young et al. (2004) detected TLR1–6 and TLR9 mRNA in both human endometrial tissues and separated endometrial epithelial cells, while Schaefer et al. (2005) demonstrated the expression of TLR1–9 mRNA in cultured human endometrial epithelial cells. An immunohistochemical study showed the presence of TLR1–6 in various locations in the human

* Corresponding author. Tel.: +81 3 3815 5411; fax: +81 3 3816 2017.
E-mail address: yutakaos-tky@umin.ac.jp (Y. Osuga).

0165-0378/$ – see front matter © 2006 Elsevier Ireland Ltd. All rights reserved.
doi:10.1016/j.jri.2006.11.004

Please cite this article in press as: Hirata, T. et al., Expression of toll-like receptors 2, 3, 4, and 9 genes in the human endometrium during the menstrual cycle, J. Reprod. Immunol. (2007), doi:10.1016/j.jri.2006.11.004

female reproductive tract, including the endometrium (Fazeli et al., 2005).

The endometrium changes its gene profile during the menstrual cycle under the influence of ovarian hormones. Accordingly, it is feasible that immunity in the endometrium alters during the menstrual cycle. However, changes of TLR expression in the endometrium during the menstrual cycle remain to be elucidated. Bacteria and viruses are common pathogens that could have contact with the endometrium. We hypothesized that proper innate immune system against these pathogens in human endometrium work with the help of TLR2, TLR3, TLR4, and TLR9 that recognize peptidoglycan from Gram-positive bacteria (Yoshimura et al., 1999), viral double-stranded RNA (Alexopoulou et al., 2001), LPS from Gram-negative bacteria (Poltorak et al., 1998) and unmethylated CpG DNA in bacterial genomes (Hemmi et al., 2000), respectively. In the present study, therefore, we have examined the gene expression profile of TLR2, TLR3, TLR4, and TLR9 through the menstrual cycle. We addressed their variation during the menstrual cycle using real-time quantitative RT-PCR and *in situ* hybridization.

2. Materials and methods

2.1. Patients and samples

Endometrial tissues were obtained from patients undergoing operations for benign gynecological conditions. All patients had regular menstrual cycles, and none had received hormonal treatment at least 6 months before surgery. Specimens were dated according to the criteria of Noyes et al. (1950) and classified as early proliferative, mid-proliferative, late proliferative, early secretory, mid-secretory, and late secretory phases. Tissues for mRNA extractions were snap-frozen in liquid nitrogen and stored at −80 °C. Tissues (5 mm × 5 mm) for *in situ* hybridization were fixed in 10% neutral buffered formalin for 16 h, stored in 70% ethanol and wax embedded. The experimental procedures were approved by the institutional review board of University of Tokyo, and signed informed consent for use of the endometrial tissue was obtained from each woman.

2.2. Isolation and culture of human endometrial stromal and epithelial cells

Isolation and culture of human endometrial stromal cells (ESC) and epithelial cells (EEC) was processed as described previously (Hirata et al., 2005; Koga et al., 2001). Fresh endometrial biopsy specimens collected in sterile medium were rinsed to remove blood cells. Tissues were minced into small pieces and incubated in DMEM/F-12 containing type1 collagenase (0.25%) and deoxynuclease1 (15 U/ml) for 120 min at 37 °C. The resultant dispersed endometrial cells were separated by filtration through a 40 μm nylon cell strainer (Becton Dickinson and Co., Franklin Lakes, NJ). Endometrial epithelial glands that remained intact were retained by the strainer, whereas dispersed ESC passed through the strainer into the filtrate.

ESC in the filtrate were collected by centrifugation, and resuspended in phenol red-free DMEM/F-12 containing 10% charcoal-stripped fetal bovine serum (FBS), 100 U/ml penicillin, 0.1 mg/ml streptomycin, and 0.25 μg/ml amphotericin B. ESC were seeded in a 100 mm culture plate and kept at 37 °C in a humidified 5% CO_2/95% air atmosphere. At the first passage, cells were plated into 12-well culture plates (Becton Dickinson and Co.) at a density of 2×10^5 cells/ml. Cells, reaching confluence in 2 or 3 days were used for the experiments.

EEC were collected by backwashing the strainer with DMEM/F-12 containing 10% charcoal-stripped FBS, seeded in a 100 mm plate and incubated at 37 °C for 60 min to allow contaminated ESC to attach to the plate wall. The non-attached EEC were recovered and cultured in the culture medium at a density of 2×10^5 cells/ml into 12-well culture plates. Cells which reached confluence in 3 or 4 days were used for experiments. The purity of both the stromal and epithelial cell preparations was more than 95% as judged by positive cellular staining for vimentin or cytokeratin, respectively.

2.3. Treatment of cells

To examine effects of hormone on TLR2, TLR3, TLR4, or TLR9 mRNA expression, EEC and ESC were incubated with 2.5% charcoal-stripped FBS in the presence of 10 ng/ml (36.7 nM) estradiol (E), 100 ng/ml (318 nM) progesterone (P), E plus P (EP), or 0.1% ethanol vehicle (control). EEC were incubated with hormone treatment for 24 and 48 h. ESC were incubated for 3, 8, 24, 48, and 72 h.

2.4. RNA extraction, RT and real-time quantitative PCR of TLR2, TLR3, TLR4, and TLR9

Using an RNeasy Mini kit (QIAGEN, Hilden, Germany), total RNA was extracted from biopsies or cultured cells. One microgram of total RNA was reverse-transcribed in a 20 μl volume using an RT-PCR kit (TOYOBO, Osaka, Japan). Standard PCR was

Please cite this article in press as: Hirata, T. et al., Expression of toll-like receptors 2, 3, 4, and 9 genes in the human endometrium during the menstrual cycle, J. Reprod. Immunol. (2007), doi:10.1016/j.jri.2006.11.004

Table 1
Primer pairs used for real-time quantitative PCR analysis

mRNA		Oligonucleotide sequences
TLR2	Sense	5′-GATGCCTACTGGGTGGAGAA-3′
	Anti-sense	5′-CGCAGCTCTCAGATTTACCC-3′
TLR3	Sense	5′-AGCCTTCAACGACTGATGCT-3′
	Anti-sense	5′-TTTCCAGAGCCGTGCTAAGT-3′
TLR4	Sense	5′-CAACAAAGGTGGGAATGCTT-3′
	Anti-sense	5′-CAACAAAGGTGGGAATGCTT-3′
TLR9	Sense	5′-GGACACTCCCAGCTCTGAAG-3′
	Anti-sense	5′-TTGGCTGTGGATGTTGTTGT-3′
GAPDH	Sense	5′-ACCACAGTCCATGCCATCAC-3′
	Anti-sense	5′-TCCACCACCCTGTTGCTGTA-3′

performed using Rever Tra Dash (TOYOBO) according to the manufacturer's instruction. Human glyceraldehyde dehydrogenase (GAPDH) primers (TOYOBO) were used to ensure RNA quality and amounts. Primer pairs of TLR2, TLR3, TLR4, and TLR9 used in PCR are shown in Table 1. Standard PCR conditions for amplifications of TLR2, TLR3, TLR4, TLR9, or GAPDH were 28 cycles (for GAPDH and TLR4) or 30 cycles (for TLR2 and TLR9) at 98 °C for 10 s, 60 °C for 2 s, and 74 °C for 15 s. PCR products were analyzed by 2% agarose gel electrophoresis. Densitometric analysis was performed using the Image J software (National Institutes of Health, Bethesda, MD, USA).

Real-time quantitative PCR was performed as reported previously (Hirota et al., 2003; Koga et al., 2000). To assess TLR2, TLR3, TLR4, and TLR9 mRNA expression, real-time quantitative PCR and data analysis were performed using Light Cycler (Roche Diagnostics GmbH, Mannheim, Germany). Expression of TLR2, TLR3, TLR4, and TLR9 mRNA was normalized to RNA loading for each sample using GAPDH mRNA as an internal standard. PCR conditions were as follows: for TLR2, 40 cycles at 95 °C for 10 s, 64 °C for 10 s, 72 °C for 12 s; for TLR3, 40 cycles at 95 °C for 10 s, 64 °C for 10 s, 72 °C for 11 s; for TLR4, 40 cycles at 95 °C for 10 s, 64 °C for 10 s, 72 °C for 11 s; for TLR9, 45 cycles, at 95 °C for 10 s, 64 °C for 10 s, 72 °C for 12 s. All PCR conditions were followed by melting curve analysis. Each PCR product was purified with a QIAEX II gel extraction kit (QIAGEN, Hilden, Germany), and their identity confirmed using an ABI PRISMTM 310 genetic analyzer (Applied Biosystems, Foster City, CA).

2.5. *In situ hybridization (ISH)*

For preparation of the dioxigenin (DIG)-labeled RNA probe for TLR2, TLR3, TLR4, and TLR9, each fragment of the human complementary DNA, obtained by RT-PCR with the primers described, was subcloned into the appropriate restriction site of the PCR2-TOPO Vector (Invitrogen, Carlsbad, CA). After linearization of the plasmid with an appropriate restriction enzyme, the linearized vectors were used as templates for the synthesis of DIG-labeled RNA probes using SP6 (antisense) or T7 (sense) RNA polymerase. *In situ* hybridization was performed using an ISHR Starting kit (Nippon Gene, Toyama, Japan) as described previously (Koga et al., 2004). Paraffin-embedded specimens were sliced at a 5 μm thickness. These sections were mounted on poly-L-lysine-treated slides, deparaffinized and rehydrated. They were further digested with 5 mg/ml proteinase K for 10 min at room temperature, treated with acetic anhydride, and then subjected to treatment with prehybridization solution for 30 min at 42 °C. Hybridization was carried out by applying the diluted probe to each slide section. Each section was incubated in a humidified chamber overnight at 42 °C. Slides were washed in washing solution at 42 °C for 20 min, treated with RNase for 30 min at 37 °C. After being blocked with blocking solution, sections were incubated with an anti-DIG alkaline phosphatase-conjugated antibody (1:500, Roche) for 1 h at room temperature. Color development was carried out by overlaying them with nitroblue tetrazolum/5-bromo-4-echoloro-3-indolyl phosphate (NBT-BCIP; Roche), and incubation in a humidified container in the dark for 8 h (TLR2 and TLR9), 10 h (TLR4), or 12 h (TLR3). Sense probe hybridization was used as a control for background level. The intensity of staining was evaluated by three independent observers using a semi-quantitative index, score = $\sum Pi$, where i is the intensity of staining with a value of 0, 1, 2, 3 (negative, weak, moderate, or strong, respectively), and P is the percentage of stained cells for each given i (range 0–100%). Staining score was the average of scores by three independent observers.

2.6. *Statistical analysis*

Expression levels of mRNA by real-time quantitative PCR and mRNA staining intensities by ISH during menstrual cycles were analyzed by Kruskal–Wallis test, followed by multiple comparisons using Dunn's procedure. Differences in the staining intensities by ISH between the epithelium and stroma in each menstrual phase were analyzed by Student's t-test. $P < 0.05$ was considered significant. Data are expressed as the mean ± S.E.M.

Please cite this article in press as: Hirata, T. et al., Expression of toll-like receptors 2, 3, 4, and 9 genes in the human endometrium during the menstrual cycle, J. Reprod. Immunol. (2007), doi:10.1016/j.jri.2006.11.004

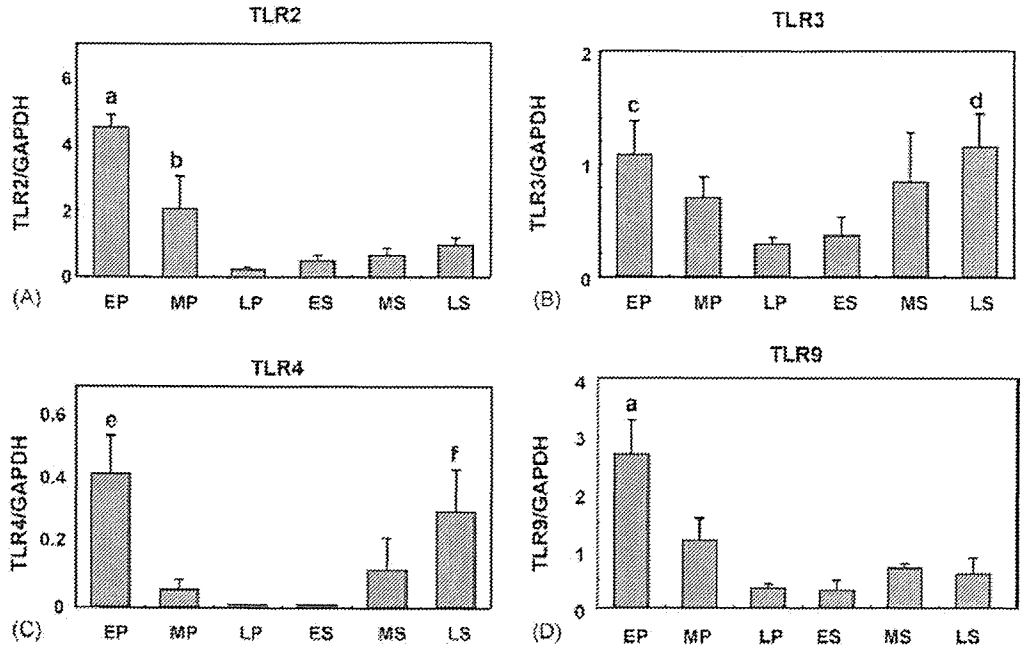

Fig. 1. Expression of TLR2 (A), TLR3 (B), TLR4 (C), and TLR9 (D) mRNA throughout the menstrual cycle. Endometrial tissues were obtained from 21 patients. The distribution according to the menstrual cycle phase was early proliferative phase (EP; $n=3$), mid-proliferative phase (MP; $n=4$), late proliferative phase (LP; $n=4$), early secretary phase (ES; $n=3$), mid-secretary phase (MS; $n=3$), late secretary phase (LS; $n=4$). The levels of TLR mRNA were determined by real-time quantitative PCR using LightCycler and normalized by those of the respective GAPDH. Data are the mean ± S.E.M. (a) $P<0.01$ vs. MP, LP, ES, MS, and LS; (b) $P<0.05$ vs. LP and ES; (c) $P<0.05$ vs. LP; (d) $P<0.05$ vs. LP and ES; (e) $P<0.05$ vs. MP, LP, ES, and MS; (f) $P<0.05$ vs. MP, LP, and ES.

3. Results

3.1. Expression of TLR2, TLR3, TLR4, and TLR9 mRNA in endometrial tissues throughout the menstrual cycle by quantitative RT-PCR

TLR2, TLR3, TLR4, and TLR9 mRNA were detected in all endometrial biopsies ($n=21$) throughout the menstrual cycle. As shown in Fig. 1, TLR2, TLR3, TLR4, and TLR9 showed significant variance during the menstrual cycle. The expression levels of all four TLRs appeared to be high at perimenstrual period and low at periovulatory period. Statistical analysis revealed the following. TLR2 mRNA expression was significantly higher in the early proliferative phase than in other phases of the menstrual cycle, and was significantly higher in the mid-proliferative phase than the late proliferative phase and early secretary phase (Fig. 1A). TLR3 mRNA expression was significantly higher in the early proliferative phase than the late proliferative phase, and was significantly higher in the late secretary phase than the late proliferative phase and early secretary phase (Fig. 1B). TLR4 mRNA expression was significantly higher in the early proliferative phase than the mid- and late proliferative phase and the early and mid-secretary phase, and was significantly higher in the late secretary phase than in the mid- and late proliferative phase and the early secretary phase (Fig. 1C). TLR9 mRNA expression was significantly higher in the early proliferative phase than other phases of the menstrual cycle (Fig. 1D).

3.2. Expression of TLR2, TLR3, TLR4, and TLR9 mRNA throughout the menstrual cycle by in situ hybridization

Fig. 2 shows the histological identification of mRNA of TLR2, TLR3, TLR4, and TLR9 in the endometrium. The TLRs examined were all expressed throughout the

Fig. 2. Localization of mRNA encoding TLR2, TLR3, TLR4, and TLR9 mRNA in human endometrium from all stages of the menstrual cycle. Endometrial tissues were obtained from 18 patients ($n=3$ in each phase). The result is representative of three samples in each phase. All TLR mRNAs were localized to the epithelial, stromal, and vascular compartment. EP, early proliferative; MP, mid-proliferative; LP, late proliferative; ES, early secretary; MS, mid-secretary; LS, late secretary; Neg, negative control treated with sense riboprobe; Vas, vascular compartments. Scale bars, 100 μm.

Please cite this article in press as: Hirata, T. et al., Expression of toll-like receptors 2, 3, 4, and 9 genes in the human endometrium during the menstrual cycle, J. Reprod. Immunol. (2007), doi:10.1016/j.jri.2006.11.004

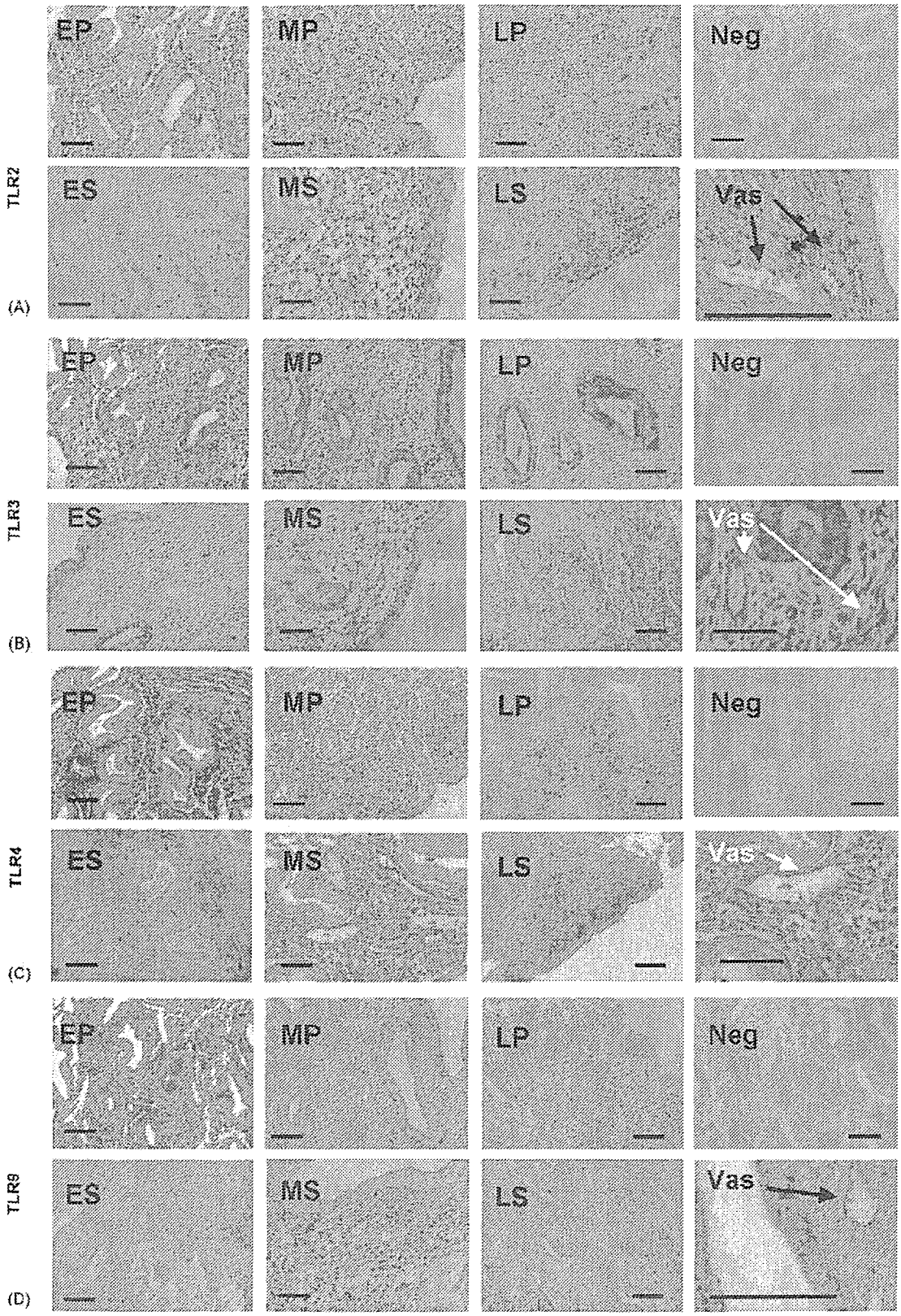

Please cite this article in press as: Hirata, T. et al., Expression of toll-like receptors 2, 3, 4, and 9 genes in the human endometrium during the menstrual cycle, J. Reprod. Immunol. (2007), doi:10.1016/j.jri.2006.11.004

menstrual cycle in both epithelial and stromal cells. No specific hybridization products were observed when using the sense riboprobes. The intensity of expression in epithelial cells and stromal cells was separately scored. Table 2 shows the summary of the results. The statistical analysis of the scores provided following findings. Expression levels were equivalent between epithelial cells and stromal cells for TLR2 and TLR9 throughout the menstrual cycle. Expression of TLR3 appeared higher in epithelial cells than stromal cells throughout the menstrual cycle, and the difference was statistically significant at the early, mid- and late secretory phase. In contrast, expression of TLR4 appeared lower in epithelial cells than stromal cells throughout the menstrual cycle, and the difference was statistically significant at the early and late proliferative, as well as early and late secretory phases. The variation of expression levels both in epithelium and stroma during the menstrual cycle appeared consistent with those observed by real-time RT-PCR.

3.3. Effects of hormone treatment on expression of TLR mRNA

The effects of hormone treatment on expression of TLR mRNA in cultured endometrial cells were then investigated. The expression of TLR2, TLR3, TLR4, or TLR9 mRNA in EEC was almost equivalent with or without hormone treatment for 24 or 48 h. The expression of TLR2, TLR3, and TLR9 mRNA in ESC were also equivalent with or without hormone treatment for 3, 8, 24, 48, and 72 h. Whereas expression of TLR4 mRNA did not significantly alter for 3, 8, 24, and 48 h, expression was significantly decreased by treatment with E, and increased by treatment with P for 72 h (Fig. 3A and B). Expression of TLR4 mRNA in ESC stimulated with P or EP was significantly stronger than in ESC stimulated with E for 72 h.

Table 2
Expression of TLRs mRNA in the endometrium determined by *in situ* hybridization

	EP	MP	LP	ES	MS	LS
TLR2						
E	++	++	+	++	++	++
S	+++	++	+	+	++	++
TLR3						
E	+++	++	++	++	++	+++
S	+++	++	+	+	++	++
TLR4						
E	++	++	+	+	+	++
S	+++	++	++	++	++	+++
TLR9						
E	+++	++	+	+	+	++
S	+++	++	+	+	++	++

E: epithelial cells, S: stromal cells +, ++, and +++ denote the average of scores <175, 175–225, and >225, respectively.

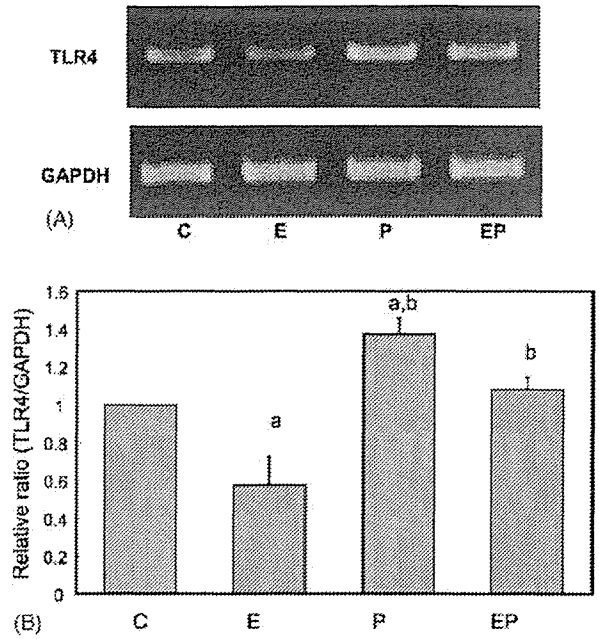

Fig. 3. (A) Effects of estradiol (E) and progesterone (P) treatment for 72 h on the expression of TLR4 mRNA. RT-PCR analysis was performed for TLR4 or GAPDH mRNA. The data shown are representative of three separate experiments using samples from different women. (B) Quantitative densitometric analysis of the expression of TLR4 mRNA. The data shown are the relative ratios (TLR4/GAPDH) measured by densitometry. Data are the mean ± S.E.M. of three independent experiments. (a) $P<0.05$ vs. control; (b) $P<0.01$ vs. E.

4. Discussion

In the present study, we have demonstrated menstrual cycle-dependent spatio-temporal gene expression of TLR2, TLR3, TLR4, and TLR9 in the human endometrium. All of these genes were expressed throughout the menstrual cycle, and alterations of the levels of expression of these four genes showed the same tendency, being high in the perimenstrual period and low in the periovulatory period. *In situ* hybridization revealed that the expression levels of TLR3 were higher in epithelial cells than in stromal cells, whereas those of TLR4 were the opposite. TLR2 and TLR9 were expressed equally in epithelial cells and stromal cells. These spatio-temporal patterns of TLR gene expression may subserve fine-tuning of innate immunity in the endometrium.

It has been reported that the proliferative phase of the menstrual cycle, especially day 1 through 7,

Please cite this article in press as: Hirata, T. et al., Expression of toll-like receptors 2, 3, 4, and 9 genes in the human endometrium during the menstrual cycle, J. Reprod. Immunol. (2007), doi:10.1016/j.jri.2006.11.004

is the primary risk factor for ascending infection by microorganisms (Eckert et al., 2002; Korn et al., 1998). Menstrual blood and shed endometrium could be a favorable environment for bacterial infection, as exemplified by toxic shock syndrome. Thus, increased expression of TLRs in the menstrual phase might be a plausible defense mechanism of the uterus.

The menstrual phase is a period when numerous white blood cells are recruited in the endometrium (Salamonsen and Woolley, 1999). White blood cells are the main source of gamma interferon in the endometrium (Yeaman et al., 1998), and gamma interferon upregulates expression of TLR4 in endometrial stromal cells (Hirata et al., 2005). Thus, leukocytes and TLRs may coordinately protect the endometrium against microbial attack.

Conversely, periovulatory low expression of TLRs might prevent unfavorable inflammatory response of the endometrium evoked by microbial contaminants with upcoming sperm (Friberg et al., 1987; Svenstrup et al., 2003). Chemical mediators, such as prostaglandins, produced by uncontrolled inflammatory responses could disturb proper uterine peristalsis for normal fecundability (Hland et al., 1997).

The variation of expression of TLRs in the endometrium appears related to alteration of ovarian hormone levels. In the present study, we have demonstrated that estradiol treatment suppressed expression of TLR4 mRNA in ESC, and progesterone treatment enhanced expression of TLR4 mRNA in ESC. However, expression TLR2, TLR3, and TLR9 mRNA in ESC as well as that of TLR2, TLR3, TLR4, and TLR9 mRNA in EEC were not affected by hormone treatment. These findings appear inconsistent with the variation of TLRs *in vivo* during the menstrual cycle. A possibility is that substances other than ovarian hormones might modulate expression of TLRs in the endometrium. Others have also reported that estradiol treatment does not alter TLR3 mRNA or protein expression in RL95-2 cells (endometrial epithelial cell line) (Lesmeister et al., 2005). A further study is warranted to reveal the regulatory mechanism for expression of TLRs in the endometrium during the menstrual cycle.

Innate immune substances other than TLRs have been shown to vary their expression levels in the endometrium during the menstrual phase. Defensins and secretory leukocyte protease inhibitor (SLPI) are bactericidal molecules secreted from endometrial cells. Human β-defensin (HBD)-3 mRNA expression is highest during the secretory phase, whereas HBD-4 mRNA peaks in the proliferative phase (King et al., 2003). The expression of SLPI is increased in endometrial epithelial cells from the mid- to late secretory phase (King et al., 2000). Many innate immune factors, including TLRs, may play individual functions depending on the phase of the menstrual cycle.

TLR3 expression was enhanced in epithelial cells compared to stromal cells. This finding is consistent with a report that TLR3 immunostaining was mainly observed in epithelial cells (Jorgenson et al., 2005). Recent studies have shown that stimulation of TLR3 in endometrial epithelial cells leads to expression of not only proinflammatory cytokines and chemokines, but also β-defensins and IFN-β, indicating prominent antiviral reactions (Schaefer et al., 2005). Thus, epithelial cells may be a premiere component against viral infection in the uterus.

TLR4, in contrast, was expressed more intensely in stromal cells. As previously demonstrated, TLR4 expression in epithelial cells was unresponsive to LPS, the ligand for TLR4, unless soluble CD14, indispensable cofactor for its activation, was supplied (Hirata et al., 2005). In contrast, stromal cells, which have membranous CD14, were responsible for LPS. The lack of membranous CD14 in epithelial cells may prevent harmful hyperresponsiveness in response to microorganisms, while stromal cells may react promptly once the epithelial barrier has been breached. Higher expression of TLR4 in stromal cells appears to be in line with the notion.

Interestingly, TLR type-dependent differential expression in distinct compartments is observed also in a longitudinal direction along with the reproductive tract. Expression of TLR2 mRNA was higher in the fallopian tube and cervical tissues than in the endometrium and ectocervix, whereas expression of TLR4 mRNA was higher in the fallopian tube and endometrium than in cervical tissues and ectocervix (Pioli et al., 2004).

In summary, we have demonstrated the variable expression of TLR2, TLR3, TLR4, and TLR9 in the human endometrium during the menstrual cycle. The overall expression patterns of these four TLRs were similarly high around menstruation and low around ovulation periods. The expression in epithelial cells and stromal cells is different depending on the TLR. The expression patterns of TLRs may subserve the fine-tuning of innate immunity in the endometrium.

Acknowledgement

This work was supported in part by Akaeda Medical Research Foundation.

Please cite this article in press as: Hirata, T. et al., Expression of toll-like receptors 2, 3, 4, and 9 genes in the human endometrium during the menstrual cycle, J. Reprod. Immunol. (2007), doi:10.1016/j.jri.2006.11.004

References

Alexopoulou, L., Holt, A.C., Medzhitov, R., Flavell, R.A., 2001. Recognition of double-stranded RNA and activation of NF-kappaB by toll-like receptor 3. Nature 413, 732–738.

Eckert, L.O., Hawes, S.E., Wolner-Hanssen, P.K., Kiviat, N.B., Wasserheit, J.N., Paavonen, J.A., Eschenbach, D.A., Holmes, K.K., 2002. Endometritis: the clinical-pathologic syndrome. Am. J. Obstet. Gynecol. 186, 690–695.

Fazeli, A., Bruce, C., Anumba, D.O., 2005. Characterization of toll-like receptors in the female reproductive tract in humans. Hum. Reprod. 20, 1372–1378.

Friberg, J., Confino, E., Suarez, M., Gleicher, N., 1987. Chlamydia trachomatis attached to spermatozoa recovered from the peritoneal cavity of patients with salpingitis. J. Reprod. Med. 32, 120–122.

Hemmi, H., Takeuchi, O., Kawai, T., Kaisho, T., Sato, S., Sanjo, H., Matsumoto, M., Hoshino, K., Wagner, H., Takeda, K., Akira, S., 2000. A toll-like receptor recognizes bacterial DNA. Nature 408, 740–745.

Hirata, T., Osuga, Y., Hirota, Y., Koga, K., Yoshino, O., Harada, M., Morimoto, C., Yano, T., Nishii, O., Tsutsumi, O., Taketani, Y., 2005. Evidence for the presence of toll-like receptor 4 system in the human endometrium. J. Clin. Endocrinol. Metab. 90, 548–556.

Hirota, Y., Osuga, Y., Yoshino, O., Koga, K., Yano, T., Hirata, T., Nose, E., Ayabe, T., Namba, A., Tsutsumi, O., Taketani, Y., 2003. Possible roles of thrombin-induced activation of protease-activated receptor 1 in human luteinized granulosa cells. J. Clin. Endocrinol. Metab. 88, 3952–3957.

Uland, M.M., Evers, J.L., Dunselman, G.A., Volovics, L., Hoogland, H.J., 1997. Relation between endometrial wavelike activity and fecundability in spontaneous cycles. Fertil. Steril. 67, 492–496.

Jorgenson, R.L., Young, S.L., Lesmeister, M.J., Lyddon, T.D., Misfeldt, M.L., 2005. Human endometrial epithelial cells cyclically express toll-like receptor 3 (TLR3) and exhibit TLR3-dependent responses to dsRNA. Hum. Immunol. 66, 469–482.

King, A.E., Critchley, H.O., Kelly, R.W., 2000. Presence of secretory leukocyte protease inhibitor in human endometrium and first trimester decidua suggests an antibacterial protective role. Mol. Hum. Reprod. 6, 191–196.

King, A.E., Fleming, D.C., Critchley, H.O., Kelly, R.W., 2003. Differential expression of the natural antimicrobials, beta-defensins 3 and 4, in human endometrium. J. Reprod. Immunol. 59, 1–16.

Koga, K., Osuga, Y., Tsutsumi, O., Momoeda, M., Suenaga, A., Kugu, K., Fujiwara, T., Takai, Y., Yano, T., Taketani, Y., 2000. Evidence for the presence of angiogenin in human follicular fluid and the up-regulation of its production by human chorionic gonadotropin and hypoxia. J. Clin. Endocrinol. Metab. 85, 3352–3355.

Koga, K., Osuga, Y., Tsutsumi, O., Yano, T., Yoshino, O., Takai, Y., Matsumi, H., Hiroi, H., Kugu, K., Momoeda, M., Fujiwara, T., Taketani, Y., 2001. Demonstration of angiogenin in human endometrium and its enhanced expression in endometrial tissues in the secretory phase and the decidua. J. Clin. Endocrinol. Metab. 86, 5609–5614.

Koga, K., Osuga, Y., Yano, T., Ikezuki, Y., Yoshino, O., Hirota, Y., Hirata, T., Horie, S., Ayabe, T., Tsutsumi, O., Taketani, Y., 2004. Evidence for the presence of angiogenin in human testis. J. Androl. 25, 369–374.

Korn, A.P., Hessol, N.A., Padian, N.S., Bolan, G.A., Donegan, E., Landers, D.V., Schachter, J., 1998. Risk factors for plasma cell endometritis among women with cervical Neisseria gonorrhoeae, cervical Chlamydia trachomatis or bacterial vaginosis. Am. J. Obstet. Gynecol. 178, 987–990.

Lesmeister, M.J., Jorgenson, R.L., Young, S.L., Misfeldt, M.L., 2005. 17Beta-estradiol suppresses TLR3-induced cytokine and chemokine production in endometrial epithelial cells. Reprod. Biol. Endocrinol. 3, 74.

Noyes, R.W., Hertig, A.T., Rock, J., 1950. Dating the endometrial biopsy. Fertil. Steril. 1, 3–9.

Pioli, P.A., Amiel, E., Schaefer, T.M., Connolly, J.E., Wira, C.R., Guyre, P.M., 2004. Differential expression of toll-like receptors 2 and 4 in tissues of the human female reproductive tract. Infect. Immun. 72, 5799–5806.

Poltorak, A., He, X., Smirnova, I., Liu, M.Y., Van Huffel, C., Du, X., Birdwell, D., Alejos, E., Silva, M., Galanos, C., Freudenberg, M., Ricciardi-Castagnoli, P., Layton, B., Beutler, B., 1998. Defective LPS signaling in C3H/HeJ and C57BL/10ScCr mice: mutations in Tlr4 gene. Science 282, 2085–2088.

Salamonsen, L.A., Woolley, D.E., 1999. Menstruation: induction by matrix metalloproteinases and inflammatory cells. J. Reprod. Immunol. 44, 1–27.

Schaefer, T.M., Fahey, J.V., Wright, J.A., Wira, C.R., 2005. Innate immunity in the human female reproductive tract: antiviral response of uterine epithelial cells to the TLR3 agonist poly(I:C). J. Immunol. 174, 992–1002.

Svenstrup, H.F., Fedder, J., Abraham-Peskir, J., Birkelund, S., Christiansen, G., 2003. Mycoplasma genitalium attaches to human spermatozoa. Hum. Reprod. 18, 2103–2109.

Takeda, K., Kaisho, T., Akira, S., 2003. Toll-like receptors. Ann. Rev. Immunol. 21, 335–376.

Yeaman, G.R., Collins, J.E., Currie, J.K., Guyre, P.M., Wira, C.R., Fanger, M.W., 1998. IFN-gamma is produced by polymorphonuclear neutrophils in human uterine endometrium and by cultured peripheral blood polymorphonuclear neutrophils. J. Immunol. 160, 5145–5153.

Yoshimura, A., Lien, E., Ingalls, R.R., Tuomanen, E., Dziarski, R., Golenbock, D., 1999. Cutting edge: recognition of Gram-positive bacterial cell wall components by the innate immune system occurs via toll-like receptor 2. J. Immunol. 163, 1–5.

Young, S.L., Lyddon, T.D., Jorgenson, R.L., Misfeldt, M.L., 2004. Expression of toll-like receptors in human endometrial epithelial cells and cell lines. Am. J. Reprod. Immunol. 52, 67–73.

Please cite this article in press as: Hirata, T. et al., Expression of toll-like receptors 2, 3, 4, and 9 genes in the human endometrium during the menstrual cycle, J. Reprod. Immunol. (2007), doi:10.1016/j.jri.2006.11.004

ELSEVIER

Journal of Reproductive Immunology
72 (2006) 85–93

JOURNAL OF REPRODUCTIVE IMMUNOLOGY

www.elsevier.com/locate/jreprimm

FR 167653, a p38 mitogen-activated protein kinase inhibitor, suppresses the development of endometriosis in a murine model

Osamu Yoshino[a], Yutaka Osuga[a,*], Kaori Koga[a], Yasushi Hirota[a], Tetsuya Hirata[a], Xie Ruimeng[a], Li Na[a], Tetsu Yano[a], Osamu Tsutsumi[a,b], Yuji Taketani[a]

[a] *Department of Obstetrics and Gynecology, Faculty of Medicine, University of Tokyo, 7-3-1, Hongo, Bunkyo-ku, Tokyo 113-8655, Japan*

[b] *CREST, Japan Science and Technology, Kawaguchi Center Building, 4-1-8, Honcho, Kawaguchi, Saitama 332-0012, Japan*

Received 4 December 2004; received in revised form 31 January 2005; accepted 15 February 2005

Abstract

In various cells including endometriotic cells, p38 mitogen-activated protein kinase (MAPK) plays essential roles for inflammation, an etiological factor for endometriosis. We evaluated the effect of FR 167653, a p38 MAPK inhibitor, on the development of endometriosis using a murine model. As an endometriosis model, estradiol-treated ovariectomized BALB/c mice were injected intraperitoneally with endometrial fragments of the syngenic donor mice. The animals were injected with either 30 mg/kg FR 167653 or only vehicle (control) s.c. twice a day, starting 2 days before endometrial injection. Three weeks later, the peritoneal fluids and the developed endometriotic lesions were collected. Both the weight of all the endometriotic lesions per mouse and the concentrations of interleukin-6 and monocyte chemoattractant protein-1 in the peritoneal fluid were significantly lower in the FR 167653-treated mice than in the control mice. These findings suggest that FR 167653 may inhibit the development of endometriosis possibly by suppressing peritoneal inflammatory status.

Keywords: Endometriosis; Animal model; P38 MAP kinase; IL-6; MCP-1; Peritoneal fluid

* Corresponding author. Tel.: +81 3 3815 5411x33407; fax: +81 3 3816 2017.
E-mail address: yutakuos-tky@umin.ac.jp (Y. Osuga).

0165-0378/$ – see front matter © 2006 Elsevier Ireland Ltd. All rights reserved.
doi:10.1016/j.jri.2005.02.004

1. Introduction

Endometriosis, defined by the presence of viable endometriotic tissue outside the uterus, is an enigmatic disease. Infertility and pain are the most common symptoms that debilitate women affected with endometriosis (Maruyama et al., 2000; Momoeda et al., 2002). Most prevalent medical therapy uses GnRH analogue, whereas its adverse effects induced by hypoestrogen often dismiss the compliance. Thus, the development of better drugs is anticipated.

Implantation and growth of endometrial cells in menstrual blood spilled into the peritoneal cavity is a widely accepted hypothetic pathogenesis. In addition, multiple lines of evidence suggest that inflammation plays a pivotal role in the pathogenesis (Harada et al., 2001; Lebovic et al., 2001). In particular, endometriotic cells and intraperitoneal leukocytes produce various proinflammatory cytokines including interleukin (IL)-6, IL-8 and monocyte chemoattractant protein (MCP)-1, which could be responsible for evoking an inflammatory environment as seen in the peritoneal cavity of women with endometriosis.

P38 mitogen-activated protein kinase (p38 MAPK), an intracellular signal-transducing molecule, plays an essential role in the expression of several inflammatory molecules in a macrophage (Matsuyama et al., 2004; Ono and Han, 2000), a central player in the pathophysiology of endometriosis. In addition, we have recently shown that an activation of p38 MAPK plays key roles in inflammatory reactions of eutopic endometrial stromal cells (Yoshino et al., 2003) and of endometriotic stromal cells (Yoshino et al., 2004).

These findings led us to speculate that inhibition of p38 MAPK might attenuate inflammation associated with endometriosis, and thereby suppress the progress of endometriosis. In the present study, we examined the effect of FR 167653, a well-characterized inhibitor of p38 MAPK (Kawano et al., 1999; Nishikawa et al., 2003; Nishikori et al., 2002; Yamamoto et al., 1996), on the induction of endometriotic lesions in a murine model.

2. Materials and methods

2.1. Animals

Female, 6–8-week-old, BALB/c mice were purchased from Tokyo Laboratory Animal Science (Tokyo, Japan). Mice were fed on mouse diet and water ad libitum and kept on a light/dark cycle of 16/8 h under controlled conditions. Prior to any invasive procedure, the mice were anaesthetized by 100 mg/kg ketamine hydrochloride (Sankyo, Tokyo, Japan) s.c. and 12 mg/kg xylazine hydrochloride (Bayer, Tokyo, Japan) s.c. All animal experiments were according to the protocol approved by the Animal Care and Use Committee of the University of Tokyo. Every surgical technique was performed under clean conditions.

2.2. Induction of endometriosis

Induction of endometriosis was performed according to the method as previously described (Dabrosin et al., 2002; Somigliana et al., 1999) with minor modifications. First,